UNIVERSIDAD NACIONAL AUTÓNOMA DE MÉXICO

PROGRAMA DE MAESTRÍA Y DOCTORADO EN INGENIERÍA
INGENIERÍA CIVIL – ESTRUCTURAS

ASSESSMENT OF THE EFFECT OF PARAMETER UNCERTAINTY IN PROBABILISTIC SEISMIC HAZARD ANALYSIS

TESIS
QUE PARA OPTAR POR EL GRADO DE:
MAESTRO EN INGENIERÍA

PRESENTA:
ALHELÍ SILVESTRE LÓPEZ CASTAÑEDA

TUTOR:
DR. ERNESTO ALFONSO HEREDIA ZAVONI

PROGRAMA DE MAESTRÍA Y DOCTORADO EN INGENIERÍA

CIUDAD DE MÉXICO, OCTUBRE DE 2017

JURADO ASIGNADO:

Presidente:	DR. LUIS ESTEVA MARABOTO
Secretario:	DR. MARIO GUSTAVO ORDAZ SCHROEDER
Vocal:	DR. ERNESTO ALFONSO HEREDIA ZAVONI
1er. Suplente:	DR. EDUARDO REINOSO ANGULO
2do. Suplente:	DR. FRANCISCO LEONEL SILVA GONZÁLEZ

Lugar donde se realizó la tesis:

FACULDAD DE INGENIERÍA, UNAM.

TUTOR DE TESIS:

_____

DR. ERNESTO ALFONSO HEREDIA ZAVONI

To my parents J. Isabel and Ma. del Rosario,
who raised me with all their love and dedication.

To my brother José Isabel, for his wise advice.

To Osvaldo and Daniel, my lifetime friends.

ACKNOWLEDGEMENTS

Firstly, I would like to express my gratitude to Dr. Ernesto Heredia Zavoni, who introduced me to this topic, for his guidance and support that ensure this master's thesis was possible. I would also like to thank my committee members, Dr. Luis Esteva, Dr. Mario Ordaz, Dr. Eduardo Reinoso and Dr. Francisco Silva for their valuable comments that helped enriched this work.

Secondly, I am grateful to the Universidad Nacional Autónoma de México for giving me the opportunity to be trained as a structural engineer in its classrooms. Special thanks to the professors and researchers from Civil Engineering for sharing their knowledge and being our guides in our academic formation.

Financial support was provided by the Consejo Nacional de Ciencia y Tecnología (CONACyT), through the Graduate Scholarship Program. Thank you for contributing to the scientific development.

Lastly, I thank my family and friends for their confidence, motivation and hope during my years here in Mexico City. Without their encouragement, I could not have done it.

ABSTRACT

In probabilistic seismic hazard analysis, some of the parameters involved in the models for magnitude distribution and ground motion intensity are estimated based on data from historical observations through a statistical inference process. This process introduces uncertainties in the estimation of these parameters and, therefore, in the seismic hazard analysis results. The interest of this work focuses on evaluating the influence of parameter uncertainty in probabilistic seismic hazard analysis. A procedure is proposed to assess the mean and variance of the annual exceedance rate of peak ground acceleration. The procedure employs a point estimate method based on the Rosenblatt transformation. Its advantage is that the number of estimating points can be readily increased if necessary. Three cases are examined for which analytical solutions are known: (1) point source with deterministic median attenuation relation, (2) point source with probabilistic attenuation relation, and (3) a circular source with probabilistic attenuation relation. Parameters from the magnitude distribution and ground motion prediction models were considered uncertain. The accuracy of the method was assessed using Monte Carlo simulations. Results indicated that the effect of parameter uncertainty can be significant for return periods of engineering interest.

RESUMEN

En el análisis probabilista de peligro sísmico, algunos parámetros que intervienen en los modelos de excedencia de magnitud y de movimiento del suelo se estiman mediante un proceso de inferencia estadística con base en datos de observaciones y registros históricos. Este proceso introduce incertidumbres en la estimación de dichos parámetros y, por ende, en los resultados del análisis de peligro sísmico. El interés de este trabajo se centra en evaluar la influencia de la incertidumbre paramétrica en el análisis probabilista de peligro sísmico. Se propone un procedimiento para estimar la media y la varianza de la tasa anual de excedencia de la aceleración máxima del suelo. El procedimiento emplea un método de estimación puntual basado en la transformación de Rosenblatt, la cual permite mapear variables físicas a un espacio de variables independientes normal estándar. Con este enfoque no se requiere utilizar momentos de orden superior de las variables aleatorias y los puntos de estimación están siempre contenidos en el dominio de las distribuciones de las variables. Se examinan tres casos de estudio con soluciones analíticas conocidas: (1) fuente puntual y relación de atenuación con mediana determinista, (2) fuente puntual y relación de atenuación probabilista, y (3) fuente extendida circular de sismicidad uniforme y relación de atenuación probabilista. Se consideraron inciertos parámetros que intervienen en los modelos de tasa de excedencia de magnitud y de intensidad de movimiento de suelo. La precisión del método se verifica mediante simulaciones de Monte Carlo. Los resultados indican que considerar la incertidumbre paramétrica tiene un efecto relevante en el cálculo de aceleraciones máximas del suelo para periodos de retorno de interés en el análisis y diseño estructural.

TABLE OF CONTENTS

LIST OF FIGURES

LIST OF TABLES

CHAPTER 1
INTRODUCTION

1.1 BACKGROUND

Essentially, probabilistic seismic hazard analysis is an approach that aims at estimating the annual probability (or rate) of exceeding some level or intensity measure of earthquake ground shaking at a site. In this analysis, some of the parameters involved in the magnitude distribution and the ground motion intensity models are estimated based on data from historical observations through a statistical inference process which introduces uncertainties. For structural safety and optimal design decision making it would be desirable to have information on the level of uncertainty involved in the estimation of seismic hazard. This thesis focuses on the assessment of the influence of parameter uncertainty in probabilistic seismic hazard analysis.

In the context of developing models for the solution of engineering problems it has been deemed convenient to classify the character of uncertainties as aleatory or epistemic. According to Der Kiureghian and Ditlevsen (2009), an aleatory uncertainty is that related to the intrinsic randomness of a phenomenon, whereas an epistemic uncertainty is the one caused by lack of knowledge or information. The Probabilistic Model Code of the Joint Committee on Structural Safety (2001) identifies uncertainties in regard to their type and origin; it differentiates between uncertainties due to inherent natural variability, model uncertainties, and statistical uncertainties. The first one is regarded as aleatory, while the latter two are considered to be epistemic uncertainties. It is understood that epistemic uncertainties can be reduced by acquiring more knowledge or information about a phenomenon, a process or a variable.

An useful framework for identifying the sources and types of uncertainties has been formulated by Der Kiureghian and Ditlevsen (2009) discussing a general model for structural reliability analysis. It involves a set of input variables $\boldsymbol{x} = (x_1, \dots, x_n)$ that take values as outcomes of a corresponding set of basic random variables $\boldsymbol{X} = (X_1, \dots, X_n)$, a parametrized probabilistic model $f_x(\boldsymbol{x}, \boldsymbol{\Theta}_f)$ describing the distribution of the random vector $\boldsymbol{X}$, and a set of parameterized physical models $y_i = g_i(\boldsymbol{x}, \boldsymbol{\Theta}_g)$, $i = 1, 2, \dots, m$, describing relations between input variables $\boldsymbol{x}$ and m derived quantities $\boldsymbol{y} = (y_1, \dots, y_m)$, which are employed in modeling the reliability problem under study. The basic variables are those that can be observed directly and, therefore, some statistics or historical data are available. The derived variables cannot be observed directly, but can be observed as a result of a laboratory experiments or field studies for model development purposes. It is now possible to identify the following sources of uncertainty:

- Uncertainty inherent in the basic random variables $\boldsymbol{X}$.
- Uncertain model error resulting from selection of the form of the probabilistic model $f_x(\boldsymbol{x}, \boldsymbol{\Theta}_f)$, used to describe the basic variables.
- Uncertain model errors resulting from selection of the physical models $y_i = g_i(\boldsymbol{x}, \boldsymbol{\Theta}_g)$, $i = 1, 2, \dots, m$, used to describe the derived variables.
- Statistical uncertainty in the estimation of parameters $\boldsymbol{\Theta}_f$ of the probabilistic model.
- Statistical uncertainty in the estimation of parameters $\boldsymbol{\Theta}_g$ of the physical model.
- Uncertain errors involved in measuring of observations, based on which parameters $\boldsymbol{\Theta}_f$ and $\boldsymbol{\Theta}_g$ are estimated.
- Uncertain errors resulting from computational errors, numerical approximations or truncations in modeling derived variables $\boldsymbol{y}$.

Uncertainties associated to human activities and decisions could be added to the uncertainties listed above. Based on the previous framework, some of the parameters estimated from observed data, which are involved in the models for the characterization of seismic hazard, can be identified as basic random variables with probability density function $f_x(\boldsymbol{x}, \boldsymbol{\Theta}_f)$, where parameters $\boldsymbol{\Theta}_f$ are obtained using an estimator $\widehat{\boldsymbol{\Theta}_f}$ through a statistical inference process. Considering the basic variables $\boldsymbol{X}$ to be random, the exceedance rate of a given ground motion intensity becomes a function of random variables and, therefore, becomes itself a random variable. The uncertainty associated with the statistical estimation of parameters $\boldsymbol{\Theta}_f$ is known as parameter uncertainty.

1.2 OBJECTIVES AND SCOPE

The main objectives of this thesis are: (1) to implement a method for assessing the uncertainty in probabilistic seismic hazard analysis due to parameter uncertainty; and (2) to evaluate the effect of parameter uncertainty on the mean and variance of the annual exceedance rate of peak ground acceleration.

The research is developed with the following scope:

i. Three case studies will be examined for which analytical solutions are available: (1) point source with deterministic median attenuation relation, (2) point source with probabilistic attenuation relation, and (3) a circular source with probabilistic attenuation relation.
ii. The parameters to be considered uncertain are the slope related parameter β of the magnitude distribution model and the standard deviation σ of the natural logarithm of the peak ground acceleration in the ground motion intensity model.
iii. The effect of parameter uncertainty will be evaluated based on the first two statistical moments of the annual exceedance rate using a point estimate method. The accuracy of the method will be validated using Monte Carlo simulations.

1.3 OUTLINE

Chapter 2 describes the mathematical formulations for three closed-form solutions of the annual exceedance rate of peak ground acceleration and a review of existing literature for characterizing the uncertainty in parameters β and σ from the magnitude distribution and ground motion intensity models. Chapter 3 describes the implementation of the point estimate method employed. Results for the case studies are then given in Chapter 4. A brief summary, the main findings, and final comments are presented in Chapter 5.

CHAPTER 2
PROBABILISTIC SEISMIC HAZARD ANALYSIS

2.1 INTRODUCTION

The methodology used in most contemporary seismic hazard analysis was first proposed by Esteva (1967) and Cornell (1968). Unlike the deterministic approach, wherein the objective is to search for a worst-case ground motion intensity, the probabilistic analysis considers all possible earthquake events and resulting ground motions, along with their associated probabilities of occurrence, in order to find the level of ground motion intensity that can be exceeded with some acceptably low rate (Baker, 2013). Probabilistic seismic hazard analysis (PSHA) provides a sound basis for representing a fairly wide range of natural variability and allows treatment of uncertainties arising from incomplete knowledge (Sen, 2009). The steps in PSHA can be summarized as follows (Baker, 2013):

i. Identify all earthquake sources capable of producing damaging ground motions.
ii. Characterize the distribution of earthquake magnitudes, i.e., the rates at which earthquakes of various magnitudes are expected to occur.
iii. Characterize the distribution of source-to-site distances associated with potential earthquakes.
iv. Predict the resulting distribution of ground motion intensity as a function of earthquake magnitude, distance, etc.
v. Combine uncertainties in earthquake size, location and ground motion intensity, using a calculation tool known as the total probability problem.

The end result of these calculations will be a full distribution of levels of ground motion intensity and their associated rates of exceedance. The key PSHA steps as outlined by Reiter (1990) are shown in Figure 2.1.

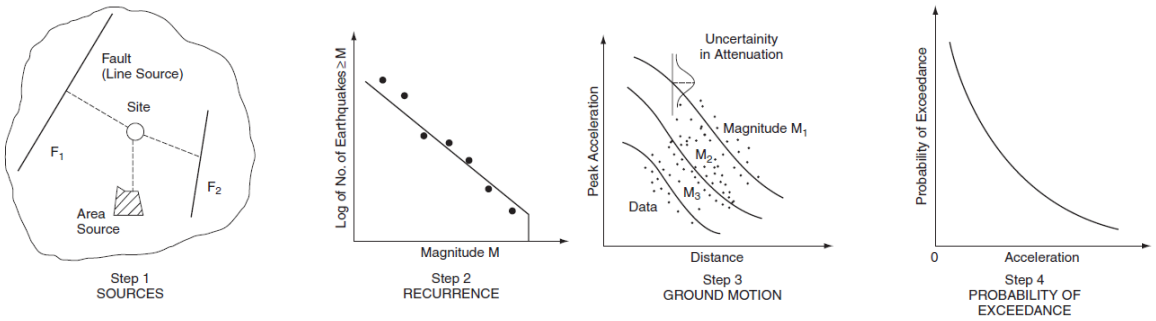

Figure 2.1 Basic steps of probabilistic seismic hazard analysis (reproduced from Sen, 2009)

2.2 ANALYTICAL SOLUTIONS FOR PSHA

Ordaz (2004) presented closed-form solutions for three simple cases of PSHA: (1) point source with deterministic median attenuation relation; (2) point source with probabilistic attenuation relation; and (3) a circular source with probabilistic attenuation relation. They are useful for prompt examinations of the variables involved and to analyze limit cases without numerical constrains; furthermore, they can also be applied as canonical solutions for more complex cases of seismic hazard analysis. The solutions were obtained for commonly used models of magnitude exceedance rates and ground motion prediction models. The mathematical formulations are described next.

The seismic activity in a source is described in terms of the magnitude exceedance rate, $\lambda(M)$, which is defined as the average annual number of earthquakes with magnitude equal or greater than M that are generated in the source. The closed-form solutions employed the modified Gutenberg-Richter model proposed by Cornell and Vanmarcke (1969), which is based on the normal Gutenberg-Richter model (Gutenberg & Richter, 1954), and defined as

$$\lambda(M) = \begin{cases} \lambda_0 \dfrac{e^{(-\beta M)} - e^{(-\beta M_U)}}{e^{(-\beta M_0)} - e^{(-\beta M_U)}}, & M_0 \le M < M_u \\ 0, & M \ge M_U \end{cases} \tag{2.1}$$

where λ_0 is the magnitude exceedance rate for $M = M_0$, β is defined as the asymptotic spectral slope at small moments, and the corresponding probability density function of magnitude takes the form

$$p(M) = \begin{cases} \dfrac{\beta e^{(-\beta M)}}{e^{(-\beta M_0)} - e^{(-\beta M_U)}}, & M_0 \le M < M_u \\ 0, & otherwise \end{cases} \tag{2.2}$$

In regard to the ground motion prediction model, Ordaz (2004) used the common assumption that the uncertain ground motion intensity, a, has a lognormal distribution with constant standard deviation of its natural logarithm equal to σ, expected value of its natural logarithm expressed as

$$E(\ln a) = a_1 + a_2 M + a_3 \ln R + a_4 R \tag{2.3}$$

and median value, $A(M, R)$, given by

$$A(M, R) = e^{E(\ln a)} = e^{a_1} e^{a_2 M} R^{a_3} e^{a_4 R} \tag{2.4}$$

where R is the source-to-site distance. The analytical solutions were developed for a single area source in terms of the intensity exceedance rate, $v(a)$, defined as the expected number of earthquakes, per unit of time, in which intensity a will be exceeded.

Case (1). Point source located at a distance R from the site and deterministic median attenuation relation. The analytical solution is

$$v(a) = \begin{cases} \lambda_0 \dfrac{\left[\dfrac{A(M_0, R)}{a}\right]^{\frac{\beta}{a_2}} - e^{(-\beta \Delta)}}{1 - e^{(-\beta \Delta)}}, & a < A(M_U, R) \\ 0, & a \ge A(M_U, R) \end{cases} \tag{2.5}$$

where

$$\Delta = M_U - M_0 \tag{2.6}$$

$A(M_0, R)$ and $A(M_U, R)$ are given by equation (2.4).

Case (2). Point source located at a distance R from the site and probabilistic attenuation relation. The analytical solution is

$$v(a) = \frac{\lambda_0}{1 - e^{-\beta\Delta}} \left\{ e^{\frac{\eta^2}{2}} \left[\frac{A(M_0, R)}{a}\right]^{\frac{\beta}{a_2}} [\Phi(Z(M_U, R) + \eta) - \Phi(Z(M_0, R) + \eta)] \right\} \tag{2.7}$$
$$+\Phi\big(Z(M_0, R)\big) - e^{-\beta\Delta}\Phi\big(Z(M_U, R)\big)$$

where

$$Z(M, R) = \frac{1}{\sigma} \ln \frac{A(M, R)}{a} \tag{2.8}$$

$$\eta = \frac{\beta\sigma}{a_2} \tag{2.9}$$

In equation (2.7), $\Phi(\cdot)$ represents the standard normal probability distribution, defined as

$$\Phi(u) = \frac{1}{\sqrt{2\pi}} \int_{-\infty}^{u} e^{\left(-\frac{x^2}{2}\right)} dx \tag{2.10}$$

Case (3). Disk source with uniform seismicity and probabilistic attenuation relation. This case is based on the geometry given in Figure 2.2, where the site of interest is located at the star, $R = (H^2 + r^2)^{\frac{1}{2}}$ and $R_0 = (H^2 + R_{\max}^2)^{\frac{1}{2}}$. The analytical solution is

$$v(a) = \frac{\lambda_0}{1 - e^{-\beta\Delta}} (K_1 T_1 + K_2 T_2 + T_3) \tag{2.11}$$

where

$$T_1 = \left(\frac{A(M_0, R_{\max})}{a}\right)^{-\frac{2}{a_3}} \begin{Bmatrix} \Phi(Z(M_0, R_0) + \gamma) - \Phi(Z(M_0, H) + \gamma) \\ -e^{-\beta'\Delta}[\Phi(Z(M_U, R_0) + \gamma) - \Phi(Z(M_U, H) + \gamma)] \end{Bmatrix}$$

$$T_2 = \left(\frac{A(M_0, R_{\max})}{a}\right)^{\frac{\beta}{a_2}} \begin{Bmatrix} \kappa^{2+\alpha}[\Phi(Z(M_0, H) + \eta) - \Phi(Z(M_U, H) + \eta)] \\ -(1 + \kappa^2)^{\frac{2+\alpha}{2}} [\Phi(Z(M_0, R_0) + \eta) - \Phi(Z(M_U, R_0) + \eta)] \end{Bmatrix} \tag{2.12a,b,c}$$

$$T_3 = (1 + \kappa^2)\Phi\big(Z(M_0, R_0)\big) - \kappa^2\Phi\big(Z(M_0, H)\big) - e^{-\beta'\Delta}\big[(1 + \kappa^2)\Phi\big(Z(M_U, R_0)\big) - \kappa^2\Phi\big(Z(M_U, H)\big)\big]$$

$$K_1 = -\frac{\alpha}{2 + \alpha} e^{\frac{2\sigma^2}{a_3^2}}; \qquad K_2 = \frac{2}{2 + \alpha} e^{\frac{\eta^2}{2}} \tag{2.13a,b}$$

$$\beta' = \beta + \frac{2a_2}{a_3}; \qquad \alpha = \frac{\beta a_3}{a_2}; \qquad \kappa = \frac{H}{R_{\max}}; \qquad \gamma = -\frac{2\sigma}{a_3} \tag{2.14a,b,c,d}$$

The analytical solution given in equation (2.11) is restricted to the case in which parameter $a_4 = 0$ (see equations (2.3) and (2.4)), i.e. a case with no anelastic attenuation.

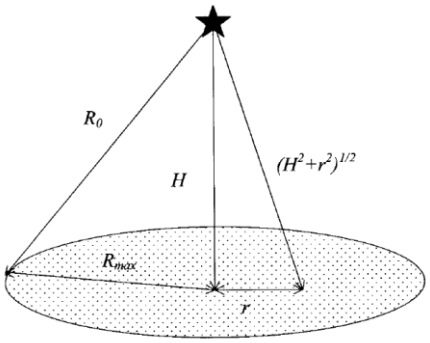

Figure 2.2 Geometry of the uniform seismicity disk source (from Ordaz, 2004)

2.3 UNCERTAIN PARAMETERS

As stated previously, some of the model parameters involved in PSHA are estimated from historical data using a statistical inference process which introduces uncertainty. According to the literature, parameters β and σ from the magnitude distribution and the ground motion intensity models, respectively, have a greater impact on the assessment of the exceedance rate of ground motion intensity. In this section, results from estimation analyses available in the literature are reviewed for the purpose of a realistic characterization of the uncertainty in these two parameters.

2.3.1 Magnitude distribution model: Parameter β

Gutenberg and Richter (1954) first described the general underlying pattern of earthquake magnitudes and occurrences. The data (distributed over a given period of time) was organized in a manner that reflected the number of earthquakes which exceeded a certain magnitude. They noted that the mean annual rate λ_M of earthquakes with magnitudes greater than M followed the relation:

$$\log_{10} \lambda_M = a - bM \tag{2.15}$$

where parameters a and b are constants for a given region. Equation (2.15) is widely known as the Gutenberg-Richter law. Parameter a represents the overall rate of earthquakes in a region, and b can be thought of as the relative likelihood of small and large magnitudes. A decrease in the value of b represents an increase in the likelihood of larger earthquakes; values of b are in the range from 0.5 to 1.5 (Dowrick, 1987).

Parameter β arises when equation (2.15) is expressed exponentially, as shown next:

$$\lambda_M = 10^{a-bM} = \exp(\alpha - \beta M) \tag{2.16}$$

where $\alpha = a \ln(10)$, and $\beta = b \ln(10)$. Parameter b can be estimated by means of least-squares regression. Estimates of b are very sensitive to the number of very large magnitude data in a given sample. For this reason, the maximum likelihood method has been suggested as a better procedure since it yields more robust estimates of b when the number of infrequent large magnitude earthquakes changes from sample to sample (Shi & Bolt, 1982).

The spatial and temporal variations of b have been studied and considered in several of the early seismicity studies. One of the pioneering works was conducted by Mogi (1962), who studied experimentally the microfracturing of rocks subjected to bending. He showed that the statistical behavior of microfracturing activity observed in laboratory experiments is similar to that observed in actual earthquakes. Modeling microfracturing as a stochastic process, he was able to describe some of the properties of the phenomenon and to relate them to the degree of heterogeneity of the material. He found that parameter b increases with the degree of heterogeneity of the rock samples and can vary widely depending on the mechanical structure of the medium and the applied stress states; for example, specimens of granite, andesite, diabase and coal, gave results equivalent to b values between 0.5 and 1.0, implying a range of β from 1.15 to 2.30.

Isacks and Oliver (1964) presented a summary of detailed regional investigations which had been carried out in southeastern California, Japan, and Central Asia, as well as less detailed investigations carried out in other regions of the world. The main result of those investigations is that the observed number of earthquakes, which occur in a given region during a certain period of time, generally fits the empirical form of equation (2.15). Parameter a exhibits a significant variation among different studies, but comparatively, b varies remarkably very little in the range from about 0.5 to 1.5, with most values between 0.7 and 1.0. Values of b from Isacks and Oliver (1964) are listed in Table 2.1. The authors noted that the apparent independence of b with respect to the region is also observed with respect to time; this can be seen in Table 2.1, where similar values of b were found for different time intervals within the same region. For relatively seismic inactive regions such as Socorro (New Mexico), the Canadian Archipelago, Fennoscandia, and the Western Rift Valley of Africa, Table 2.1 shows that b estimates are equal to 1.0, 0.83, 0.84, and 0.6, respectively. Based on the results reported by Isacks and Oliver (1964), Cornell (1968) considered that values of the parameter β may vary from 1.5 to 2.3.

Assuming that magnitude data are random samples from a population following the Gutenberg-Richter relation, it has been shown that both the method of moments (Utsu, 1965) and the method of maximum likelihood (Aki, 1965) yield the following estimator of parameter b:

$$\hat{b} = \frac{\log_{10} e}{\overline{M} - M_{min}} \tag{2.17}$$

where M_{min} is a threshold magnitude above which the data is complete, $\overline{M}$ is the sample mean of earthquake magnitude $M \geq M_{min}$, and $\log_{10} e = 0.434294$. The standard deviation of the maximum likelihood estimator of b is approximately equal to $b/\sqrt{N}$ for large N (the number of earthquakes of $M \geq M_{min}$). The estimator of b follows the χ^2 distribution and the statistical significance of the difference in the b value, for two different earthquake groups, can be tested by the F-distribution (Utsu, 1966). Since equation (2.17) is defined for a continuous exponential distribution of magnitude M, care must be taken when using discrete (rounded) magnitude values. In a later work, Utsu (2002) reported that numerous studies indicate that the Gutenberg-Richter relation is approximately valid in most cases and the value of b falls in the range of 0.6 to 1.1, i.e. β varies from about 1.38 to 2.53.

Shi and Bolt (1982) studied the uncertainties in the estimates of b. For large samples and slow temporal variations of b, they expressed the standard deviation of $\hat{b}$ as

$$\sigma(\hat{b}) = 2.030 b^2 \sigma(\overline{M}) \tag{2.18}$$

where $\overline{M}$ is the sample mean magnitude, $\sigma^2(\overline{M}) = \sum_{i=1}^{n} (M_i - \overline{M})^2/(n(n-1))$ is the sample variance of magnitudes M_i, and n is the number of sample data. The authors presented convenient tables for the standard error that allowed performing statistical tests of both temporal and spatial variations of b. The

seismicity of central California was analyzed in their work utilizing a catalog from 1952 to 1978. It was reported that, over the entire time interval, the sample average of b and 90% confidence limits are equal to $0.95\ (-0.30, +0.94)$. Within the 90% confidence limits, b varies from a low value of $0.60\ (-0.09, +0.11)$ in 1955 to a high value of $1.39\ (-0.21, +0.25)$ in 1967.

Table 2.1 Values of *b* for various regions (from Isacks and Oliver, 1964)

Reference	Region and Time Interval	No. of Eqs.	Magnitude Range	Magnitude Measure [1]	Observed Slope	+*b* [(2)]
Richter, 1958 (Gutenberg and Richter, 1954)	Entire world 1918-1955, M > 7; 1935-1938, M = 6 - 7	1190	6 – 8 ½	Ms		1.00
Gutenberg and Richter, 1954	Alaska	58	6 – 8	Ms		1.10
	Mexico, Central America	52	6 – 8	Ms		0.90
	South America	34	6 – 8	Ms		0.45
	Kermadec & Tonga	22	6 – 8	Ms		1.20
	Solomon Islands	54	6 – 8	Ms		1.00
	Sunda	36	6 – 8	Ms		0.90
	Pamir, E. Asia	27	6 – 8	Ms		0.60
	Atlantic Ocean	27	6 – 8	Ms		1.40
	Indian Ocean	19	6 – 8	Ms		1.30
Richter, 1958	Southern California:					
	Jan 1934 – May 1943	462	4 – 7	ML, n		0.85
	Jan 1953 – June 1956	530	3 – 6	ML, n		0.90
Richter, 1958	New Zealand Oct 1940 – Jan 1944	232	4 – 8	ML, n		0.90
Bune *et al.*, 1960	Garm Region, Tadzhik SSR, 1955 – 1956	2500	1 – 5	$\log_{10} E$, n	0.43	(0.80) [3]
	Chusal Section of Garm Region, 72 hrs. observation	326	-1 -+ 2	$\log_{10} E$, o	0.47	(0.80) [3]
Bune, 1961	Staliband Region of Tadzhik SSR:					
	Jan 1955 – June 1957	(250)	2 – 3 ½	$\log_{10} E$, n	0.47	(0.80)
	July 1957 – Dec 1959	(250)	2 – 3 ½	$\log_{10} E$, n	0.43	(0.80)
	1955 – 1959	(500)	2 – 3 ½	$\log_{10} E$, n	0.45	(0.80)
	1929 – 1959	(3000)	2 – 4 ½	$\log_{10} E$, ?	0.45	(0.80)
Kawasumi, 1952a	Japan, 1904 – 1943	383	5 – 7	Mk, n	0.54	(1.10) [4]
Tsuboi, 1957	Japan, 1931 – 1955	382	6 – 8	ML, n		0.70 (0.90) [5]
Gutenberg and Richter, 1954	Japan, 1904 – 1945, M 7 ¾ 1922 – 1945, M = 7 - 7.7 1932 – 1935, M = 6 – 7	101	6 – 8	Ms		0.90
Ishimoto and Iida, 1939	Kwanto Region, Japan, 1935 – 1938	1635		A, n	1.74	0.70
Kawasumi, 1952b	Kwanto Region, Japan, 1911 – 1940	1847	3 ½ - 6.0	Mk, n	0.56	(1.10) [4]
Suzuki, 1959	Kwanto Region, 1932 – 1941	519	3.5 – 5.5	A, n	1.51	0.50
Asada, 1957	Kwanto Region: 48 hrs. observation at Mt. Tsukuba	276	-1 -+ 0.5	A, o	1.88	0.90
Asada, Suyehiro, and Aakamatu, 1958	Matsushiro, Japan: 45 hrs. observation	132	-1 – 0.0	A, o	1.80	0.80

Table 2.1 – Continued

Reference	Region and Time Interval	No. of Eqs.	Magnitude Range	Magnitude Measure [1]	Observed Slope	$+b$ [(2)]
Suzuki, 1959	Aftershocks of Japanese Eq.:					
	1927 Tango Eq.	1161	2 – 4.5	A, n	1.95	0.95
	1945 Nankai Eq.	261	2 – 4.5	A, n	1.82	0.80
	1948 Fukui Eq.	541	2 – 4.5	A, n	1.86	0.90
	1948 Fukui Eq. 15 hrs	262	-1 -+ 0.5	A, o	1.87	0.90
	1949 Imaichi Eq.	148	2 – 4.5	A, n	1.79	0.80
	1949 Imaichi, 18 hrs.	623	-1 -+ 0.5	A, o	1.70	0.70
Richter, 1958	Aftershocks of 1952 Kern Co. Eq.	427	3 – 6	ML, n		0.90
Båth and Beinoff, 1958	Aftershocks of 1952 Kanchatka Eq.	409	6 – 7.5	Mb	1.5	(0.90) [6]
Utsu, 1962	Aftershocks of					
	1957 Aleutian Eq.	650	4 ¾ - 7 ¼	Mb, o		0.70
	1958 C. Alaskan Eq.	900		Mb, o		0.90
	1958 SE Alaskan Eq.	300		A, o		0.90
Mei, 1960	China, 50 years	311	5.5 – 8.5	I		0.60
Karnik, 1961	Europe, 1901 – 1955	3396	5 – 7	I	0.47	0.70
Sutton and Berg, 1958	Western Rift Valley, Africa: May 1953 – April 1956	234	3 – 6.5	ML, n		0.60
Sykes, 1963 [7]	Canadian Archipelago: Nov 1957 – Dec 1962	264	1 – 4	ML, o		0.83
Miyamura, 1962a and Båth, 1953, 1956	Fennoscandia 1891 – 1950	1043	2.5 – 6	I		0.54
Sanford and Holmes 1962	Socorro, New Mexico area: Jan 1955 – Aug 1953	173	-2 – 0	$\log_{10} E$, o		(1.0) [8]

Notes on table:

[1] The following abbreviations are used in the "Magnitude Measure" column: Ms — Gutenberg and Richter surface wave magnitude scale; ML — Richter local magnitude scale; $\log_{10} E$ — logarithm of calculated energy, used in Russian Tadzhikistan expedition; Mk — intensity scaled used by Kawasumi; A — maximum trace amplitude on seismogram; Mb — Gutenberg body wave magnitude scale; I — intensity data; n — magnitude measure based on data from more than one station in region; o — data from only one station used.

[2] Numbers in paretheses are calculated by Isacks and Oliver from data in reference.

[3] Bune (1960) gives $d(\log_{10} E)/d(ML) = 1.8$.

[4] Kawasumi (1956) gives $d(Mk)/d(Ms) = 2.0$.

[5] Tsuboi appears to have given undue weight to data points representing low earthquake counts; a replot of his data gives a better fit for $b = 0.9$.

[6] Richter (1958) gives $d(Mb)/d(Ms) = 0.63$.

[7] Personal communication from L. R. Sykes; data from Bulletins (Seismological Series) of the Dominion Observatories, Ottawa, Canada.

[8] b value listed corresponds to — $d(\log_{10} N)/d(\log_{10} SV_{\max})$ where $SV_{\max}$ is the computed amplitude at 1 km from the focus.

Bender (1983) compared estimates of b applying fitting techniques such as interval and cumulative least squares formulas, minimum χ^2 formula, and maximum likelihood formulas for continuous and interval magnitude data, to sets of N simulated magnitudes generated using random numbers for two populations with b values equal to 0.6 and 1.0. She concluded that considerably different estimates can be obtained from the same data sample because of: (1) different assumptions regarding maximum magnitude and the techniques for dealing with magnitude interval size; (2) zero observations in any magnitude interval; and (3) influence of large magnitude earthquakes. The maximum likelihood formula for grouped data can properly account for maximum magnitude, interval size, and intervals with zero observations, whereas

the maximum likelihood formulas for continuous data give b estimates which are almost identical to those obtained using the grouped data formula if the magnitude interval is small ($\Delta M = 0.1$). Bender pointed out that estimates of b should never be trusted unless N is large enough, and that at least 25 earthquakes are required to obtain an estimate of b with a standard deviation as low as $\sigma_b <\approx 0.25b$. For $N = 100$ the standard deviation of the estimate is $\approx 0.1b$ and becomes significantly higher as the sample size decreases.

In the last two decades, there have been numerous regional studies on estimation of b around the world with results published in several scientific papers. Stirling et al. (2000) carried out a seismic hazard study of New Zealand, for which the country was divided into 14 shallow and 23 deep seismicity zones, across which b values for the distributed seismicity were found to vary from 0.82 to 1.34, with an average of about 1.1, i.e., an average β about 2.53.

Grünthal and Wahlström (2001) investigated the sensitivity of different parameters used in a probabilistic seismic hazard calculation by different logic tree runs with alternative magnitude sets, source zone models and attenuation relations, with different sets of values of seismicity parameters. They reported that typical β values are in the range from 2 to 2.5 and concluded that for greater values of β (smaller fraction of large events) seismic hazard is lower, with such effect being virtually stable over a wide range of hazard levels.

Kagan (2002) discussed various theoretical statistical distributions of seismic moment data and applied them to estimate distribution parameters of magnitude. In this work, the moment magnitude, m, is defined as

$$m = (2/3)(\log_{10} M - 6) \tag{2.19}$$

where M is the scalar seismic moment (in newton meter) and the original Gutenberg-Richter law (see equation (2.15)) is transformed into the Pareto distribution for the scalar seismic moment, as

$$f(M) = \beta_{\mathrm{K}} M_t^{\beta_{\mathrm{K}}} M^{-1-\beta_{\mathrm{K}}}, \quad M_t \leq M \tag{2.20}$$

where M_t is a magnitude distribution threshold from the left, and $\beta_{\mathrm{K}} = \frac{2}{3}b$ is the index parameter of the distribution. Since the distribution density tail has a decline stronger than $M^{-1-\beta_{\mathrm{K}}}$ with β_{K}>1, the author modified the Pareto distribution in equation (2.20) at the large size end of the moment scale introducing into the distribution an additional parameter called the maximum or corner moment. In this manner, in addition to the Pareto distribution, the next four distributions were considered in order to approximate the seismic moment data: (a) the characteristic distribution; (b) the truncated Pareto or Gutenberg and Richter distribution; (c) the tapered Pareto (Gutenberg and Richter) distribution (TGR); and (d) the gamma distribution. The maximum likelihood method was employed to estimate the seismic moment distribution parameters (such as the maximum or corner moment and β_{K}) from catalogue data, for one-parameter and two-parameter estimation. To evaluate the accuracy of the procedures, the author employed a simulation technique to estimate some statistics; only the results for TGR distribution were presented, for which synthetic values of the seismic moment were generated and applied to the one-parameter and two-parameter estimation. The uncertainties of the relevant parameters were evaluated in terms of standard errors. Results for statistics of β_{K} for one-parameter and two-parameter estimation based on simulated catalogues are shown in Table 2.2 and Table 2.3, respectively. Comparing Table 2.2 and Table 2.3 shows that β_{K} estimates in the one-parameter estimation have a slightly greater standard error. The author indicated that the β_{K} estimates and their standard errors for the two-parameter case are smaller than those obtained using the maximum likelihood method, due that the large events have been removed in the former case. Using the Harvard catalogue data, the author compared the moment

distribution parameters for various periods, for different tectonic provinces and depth ranges, and for earthquakes with various focal mechanisms, concluding from the statistical analysis that $\beta_{\mathrm{K}} = 0.63$ can be considered universal for moderate earthquakes ($\beta_{\mathrm{K}} = 0.60 - 0.65$), i.e., converting the index parameter distribution used in this work, $\beta_{\mathrm{K}} = \frac{2}{3} b = 0.63$, to $\beta = b \ln 10$ we obtain that $\beta = 2.18$.

Table 2.2 β_{K}-values and their errors in simulated catalogues; one-parameter estimation (from Kagan, 2002)

No.	n	$\hat{s}_c \pm \sigma_s$	$\hat{\sigma}_s$	$\breve{\beta}_{\mathrm{K}} \pm \sigma_{\beta_{\mathrm{K}}}$	$\hat{\eta} \pm \sigma_\eta \times 0.001$	G-R Prob
1	5000	1.996 ± 0.053	0.053	0.661 ± 0.012	1.030 ± 0.191	1.00
2	2500	1.993 ± 0.076	0.075	0.661 ± 0.018	1.061 ± 0.283	1.00
3	1000	1.982 ± 0.119	0.118	0.661 ± 0.028	1.158 ± 0.498	1.00
4	750	1.976 ± 0.136	0.135	0.662 ± 0.032	1.214 ± 0.607	0.98
5	500	1.964 ± 0.165	0.162	0.662 ± 0.039	1.335 ± 0.833	0.78
6	250	1.928 ± 0.225	0.219	0.663 ± 0.055	1.736 ± 1.575	0.29
7	100	1.832 ± 0.321	0.301	0.666 ± 0.089	3.291 ± 4.561	0.09
8	50	1.708 ± 0.398	0.358	0.671 ± 0.127	6.726 ± 11.38	0.07

n, the number of events, $\hat{s}_c \pm \sigma_s$, simulated average reduced corner magnitude and its standard deviation, using eq. (31) (Kagan, 2002); $\hat{\sigma}_s$, average standard deviation, using eq. (34) (Kagan, 2002); $\breve{\beta}_{\mathrm{K}} \pm \sigma_{\beta_{\mathrm{K}}}$, β_{K}-value and its confidence limits, using eq. (24) (Kagan,2002), β_{K} is measured between $s = 0$ and $s_u = 1.5$; $\hat{\eta} \pm \sigma_\eta$, reciprocal of the reduced corner moment and its standard deviation; 'G-R Prob', the probability of the G-R law to be rejected at the 95 per cent confidence level.

Table 2.3 β_{K}-values and their errors in simulated catalogues; two-parameter estimation (from Kagan, 2002)

No.	n	S_{c}	$\breve{s}_c \pm \sigma_s$	$\breve{\beta}_{\mathrm{K}} \pm \sigma_{\beta_{\mathrm{K}}}$	$\hat{\sigma}_s$	$\hat{\sigma}_{\beta_{\mathrm{K}}}$	ρ	ν_{c}
1	5000	1000.00	1.966 ± 0.055	0.667 ± 0.010	0.055	0.010	0.24	18.41
2	2500	1000.00	1.992 ± 0.078	0.666 ± 0.014	0.078	0.014	0.24	9.21
3	1000	1000.00	1.981 ± 0.122	0.666 ± 0.022	0.122	0.022	0.25	3.68
4	500	1000.00	1.962 ± 0.170	0.665 ± 0.031	0.169	0.032	0.25	1.84
5	250	1000.00	1.925 ± 0.230	0.662 ± 0.044	0.228	0.045	0.26	0.92
6	100	1000.00	1.823 ± 0.326	0.655 ± 0.071	0.322	0.072	0.29	0.37
7	1000	3162.28	2.293 ± 0.174	0.666 ± 0.022	0.171	0.022	0.18	1.71
8	1000	1000.00	1.981 ± 0.122	0.666 ± 0.022	0.122	0.022	0.25	3.68
9	1000	316.23	1.658 ± 0.086	0.666 ± 0.024	0.086	0.023	0.34	7.95
10	1000	100.00	1.329 ± 0.062	0.666 ± 0.026	0.062	0.026	0.45	17.25
11	1000	31.62	0.998 ± 0.047	0.665 ± 0.031	0.047	0.031	0.59	37.97

n, the number of events; S_{c}, the input corner moment used in simulations; $\breve{s}_c \pm \sigma_s$, simulated average reduced corner magnitude and its standard deviation; $\breve{\beta}_{\mathrm{K}} \pm \sigma_{\beta_K}$, the same as for β_{K}-value; $\hat{\sigma}_s$, $\hat{\sigma}_{\beta_{\mathrm{K}}}$, and ρ are the average values of a correlation matrix components (see the Appendix (Kagan, 2002)); ν_{c}, the number of events larger than s_{c}, eq. (47) (Kagan, 2002).

Bird and Kagan (2004) used a new plate model to analyze the mean seismicity of seven types of plate boundaries. As part of the process, shallow earthquakes were classified into eight sub-catalogues, which correspond to seven types of plate boundaries and plate interiors. Each sub-catalogue was analyzed by

maximum likelihood methods to determine the parameters of a tapered Gutenberg and Richter relation (Kagan, 2002). In this work the conversion $m = (2/3)(\log_{10} M - 9.05)$ of Hanks and Kanamori (1979) was used, where M is the scalar moment, m is the moment magnitude, and $\beta_{\mathrm{K}} = \frac{2}{3} b$ is defined as the asymptotic spectral slope at small moments. They found variations in the maximum likelihood estimations of β_{K} from 0.53 to 0.92, but all 95% confidence intervals were consistent with a common range from 0.61 to 0.66, i.e., β ranges from 2.11 to 2.28. Table 2.4 shows the results of the maximum likelihood analysis. In addition, results were reported for five alternative sets of Monte Carlo sub-catalogues that allowed to test the sensitivity of all the results to residual uncertainties in classification (due to the algorithms performed for the shallow earthquakes classification), see Table 2.5.

Table 2.4 Tapered Gutenberg-Richter frequency-magnitude parameters of the maximum-probability sub-catalogues (from Bird and Kagan, 2004)

Catalogs	Class									
	CRB Continental Rift Boundary	CTF Continental Transform Fault	CCB Continental Convergent Boundary	OSR Oceanic Spreading Ridge		OTF Oceanic Transform Fault, by Plate Velocity, (mm/a)			OCB Oceanic Convergent Boundary	SUB SUB-duction Zone
				Normal	Other	3 – 39	40 – 68	69 – 263		
Harvard CTM Catalog (01/01/77 – 09/30/02)										
Threshold, M_t, N·m	1.13×10^{17}	3.5×10^{17}	3.5×10^{17}	1.13×10^{17}			2×10^{17}		3.5×10^{17}	
All earthquakes*	353*	272*	357*	458*	77*	428.0*	447.0*	416.0*	119*	2723*
Excluding orogens	286	198	274	422	64	400	413	385	105	2049
Slope, β_{K}	0.65 ± 0.11	0.65 ± 0.12	0.62 ± 0.10	0.93 0.61 – 1	0.82 0.58 – 1	0.64 ± 0.08	0.65 ± 0.11	0.71 ± 0.11	0.51 0.39 – 0.66	0.64 ± 0.04
Corner magnitude, m_{c}	7.30 6.90 - ?	8.02 7.52 - ?	7.48 7.18 - ?	5.87 5.7 – 6.04	7.40 6.68 - ?	7.98 7.42 - ?	6.57 6.4 – 6.84	6.63 6.46 – 7.01	7.77 7.42 - ?	8.20 7.96 – 9.10
Pacheco and Sykes [1992] catalog (1900-1975) and *Ekström and Nettles* [1997] catalog (1976): $M_s \geq 7$										
Threshold, M_t, N·m				5.1×10^{19}						
All earthquakes*	10*	42*	32*	1*		7*	1*	3*	21*	275*
Excluding orogens	9	30	19	1		7	1	3	18	218
Three catalogs merged (1900 – 2002): $M_s \geq 7$										
Threshold, M_t, N·m				5.1×10^{19}						
All earthquakes*	11*	51*	45*			11*			28*	389*
Slope, β_{K}	0.65†	0.65†	0.62†			0.64†			0.51†	0.64†
Corner magnitude, m_{c}	7.60* 7.34 – 8.42	8.03* 7.81 – 8.50	8.43* 8.03 - ?			8.12* 7.73 - ?			8.03* 7.82 – 8.51	9.58* 9.12 - ?

*Including earthquakes in the 13 orogens.
†From CMT results
All ranges are 95% confidence limits

Table 2.5 Tapered Gutenberg-Richter frequency-magnitude parameters from mean of five sets of Monte Carlo sub-catalogues (from Bird and Kagan, 2004)

Catalogs	Class									
	CRB Continental Rift Boundary	CTF Continental Transform Fault	CCB Continental Convergent Boundary	OSR Oceanic Spreading Ridge		OTF Oceanic Transform Fault, by Plate Velocity, (mm/a)			OCB Oceanic Convergent Boundary	SUB SUB-duction Zone
				Normal	Other	3 – 39	40 – 68	69 – 263		
Harvard CTM Catalog (01/01/77 – 09/30/02)										
Threshold, M_t, N·m	1.13×10^{17}	3.5×10^{17}	3.5×10^{17}	1.13×10^{17}		2×10^{17}			3.5×10^{17}	
All earthquakes*	347.2*	280.6*	320.4*	463.8*	104.6*	421.6*	431.8*	398.2*	148.0*	2733.4*
Excluding orogens	285.8	199.0	244.8	426.6	88.2	396.0	400.8	368.2	130.4	2056.6
Slope, β_K	0.64 ± 0.10	0.64 ± 0.12	0.61 ± 0.10	0.91 0.59–1	0.82 0.61 – 1	0.63 ± 0.08	0.64 ± 0.11	0.76 ± 0.11	0.54 ± 0.13	0.64 ± 0.04
Corner magnitude, m_c	7.44 7.02 - ?	8.01 7.50 - ?	7.48 7.18 - ?	5.85 5.7 – 6.05	7.38 6.71 - ?	7.38 7.42 - ?	6.53 6.37 – 6.79	7.14 6.76 – ?	7.77 7.41 - ?	8.21 7.97 – 9.10
Pacheco and Sykes [1992] catalog (1900-1975) and *Ekström and Nettles* [1997] catalog (1976): $M_s \geq 7$										
Threshold, M_t, N·m				5.1×10^{19}						
All earthquakes*	12.8*	39.6*	31.4*	1.6*		5.2*	3.4*	4.4*	21.8*	272.0*
Excluding orogens	10.0	30.6	19.2	1.6		5.2	3.4	4.2	19.2	214.2
Three catalogs merged (1900 – 2002): $M_s \geq 7$										
Threshold, M_t, N·m				5.1×10^{19}						
All earthquakes*	14.2*	49.6*	44.2*			7.8*			29.6*	384.0*
Slope, β_K	0.64†	0.64†	0.61†			0.63†			0.54†	0.64†
Corner magnitude, m_c	7.68* 7.43 – 8.40	7.99* 7.78 – 8.46	8.50* 8.12 - ?			8.16* 7.72 - ?			8.06* 7.82 – 8.62	9.58* 9.13 - ?

*Including earthquakes in the 13 orogens.
†From CMT results
All ranges are 95% confidence limits

González de Vallejo et al. (2006) conducted the first probabilistic seismic hazard analysis of The Canary Islands. The Cornell (1968) approach was used considering three seismogenic sources. The analysis assumes that earthquake occurrence follows a Poisson process and it is uniformly distributed within the source zones. In each zone, earthquake magnitudes fit an exponential distribution and the magnitude distribution follows the expression proposed by Cornell and Vanmarcke (1969) given in equation (2.1). The estimates of parameter b for each zone using regression analysis are shown in Table 2.6, with indication of the standard error. From Table 2.6 one can observe that b ranges from 0.95 to 1.12, meaning that β is about 2.18 to 2.56.

Table 2.6 Seismic parameters of the seismogenic zones (from González de Vallejo et al., 2006)

Sources	b	a	m_0	λ_{m_0}	m_1	MRP (years)
Zone 1	1.12 (± 0.01)	3.72 (± 0.05)	4.0	0.1676	6.0	1050 ± 120
Zone 2	0.95 (± 0.08)	2.75 (± 0.23)	4.0	0.0909	6.0	870 ± 160
Zone 3	1.12 (± 0.01)	3.72 (± 0.05)	6.0	0.00095	6.8	8350 ± 950

a and b, Gutenberg-Richter parameters with indication of the standard error; m_0 and m_1, lower and upper bounds of magnitude (M_w) distribution; λ_{m_0}, mean annual cumulative rate of magnitude $\geq m_0$; MRP, mean recurrence period of m_1 in each of the zones. See text for discussion (González de Vallejo, et al., 2006).

Focusing on a preliminary review of the seismic hazard in Chile, Leyton et al. (2009) used a probabilistic approach considering two main seismogenic sources: interplate thrust earthquakes and intraplate intermediate depth earthquakes. Combining the information from three seismic catalogues they defined linear relations between surface magnitude, M_S, and different earthquake magnitudes used in Chile in order to get a homogenous data catalogue and be able to estimate the Gutenberg and Richter model parameters using the maximum likelihood method. The results are shown in Table 2.7 for all the seismogenic sources considered. One can observe from the reported results that estimates of b are in the range from 0.63 to 1.08, and thus, β is about 1.45 to 2.49.

Table 2.7 Estimated parameters of the Gutenberg and Richter relation (from Leyton et al., 2009)

	Zone						
Parameter	Z1	Z2	Z3	Z4	Z5	Z6	Z7
a	4.89	5.65	4.62	6.43	5.2	5.37	5.94
b	0.63	0.75	0.7	1.08	0.68	0.82	0.94

2.3.2 Ground motion prediction model: Parameter σ

The ground motion prediction models, also known as attenuation relations, characterize the probability distribution of ground motion intensity as a function of earthquake magnitude, distance, faulting mechanism, near-surface site conditions, directivity effects, etc. These models are generally developed using statistical regression on observations from ideally large catalogues of observed ground motion intensities, and take the following general form:

$$\ln IM = \overline{\ln IM}\,(M, R, \theta) + \sigma(M, R, \theta) \cdot \varepsilon \tag{2.21}$$

where $\ln IM$ is the natural logarithm of the ground motion intensity measure of interest, e.g. peak ground acceleration or spectral acceleration at a given period, which is modeled as a random variable. In the right hand side of equation (2.21), $\overline{\ln IM}\,(M, R, \theta)$ and $\sigma(M, R, \theta)$ are the predicted mean and standard deviation of $\ln IM$, respectively. These are functions of earthquake magnitude M, source-to-site distance R, and other parameters θ. ε is the standard normal random variable that represents the observed variability in $\ln IM$ (Baker, 2013). Sen (2009) reported that the variation of the ground motion parameters with M and R are lognormally distributed.

Both the ground motion prediction models and their associated σ values are of great importance for the study of seismic hazard. Over decades of development, the prediction models have become more

complex and many authors have reported considerable scatter in the data. A certain amount of scatter is inevitable as not enough is known about the source, travel path and local site conditions (Sen, 2009). Strasser et al. (2009) refer to the scatter associated with ground motion prediction equations as an aleatory uncertainty of ground motion. After a detailed literature review, Wang (2010) summarizes, in his words, that "the standard deviation σ is a key parameter that influences hazard calculation, and becomes a critical parameter at low probabilities of exceedance in particular" and that "σ becomes so important in PSHA that much effort has been dedicated to the study of σ, including how to split into aleatory and epistemic uncertainty, or how to quantify uncertainty of uncertainty".

An early attempt of an attenuation relationship, relating magnitude and distance, was suggested by McGuire (1974), as follows:

$$\log_{10} y = b_1 + b_2 M - b_3 \log_{10}(R + 25) \tag{2.22}$$

The coefficients of equation (2.22) for peak ground displacement, velocity and acceleration are shown in Table 2.8.

Table 2.8 Coefficients for McGuire's Attenuation Relationship (1974)

	b_1	b_2	b_3	Coeff. of var. of y
a (cm/sec^2)	2.649	0.278	1.301	0.548
v (cm/sec)	0.714	0.401	1.202	0.696
d (cm)	-0.460	0.434	0.885	0.883

Cornell et al. (1979) proposed the following predictive model for lognormally distributed peak ground acceleration (in units g) with mean given by

$$\overline{\ln PGA} = -0.152 + 0.859M - 1.803\ln(R + 25) \tag{2.23}$$

and constant standard deviation of ln PGA equal to 0.57 for all magnitudes and distances.

Ordaz et al. (1989) assessed the seismic risk in the state of Guerrero, Mexico. The elastic response spectrum pseudo-accelerations, for 5% critical damping, were chosen as the ground motion intensity for deriving attenuation laws in terms of magnitude and seismic focal position. Two different attenuation laws were developed, one for shallow earthquakes ($H \leq 50$ km) and one for deep focus earthquakes ($H > 50$ km). In the case of shallow earthquakes, a regression analysis was performed from the available data of far-field accelerations. The following expressions were reported:

$$E(\log_{10} a_{\max} | M, R_0) = \min(A_c, 1.76 + 0.3M - \log_{10} R_0 - 0.0021 R_0) \tag{2.24}$$

$$\sigma(\log_{10} a_{\max} | M, R_0) = 0.25 \tag{2.25}$$

where $E(\cdot)$ and $\sigma(\cdot)$ are the expected value and the standard deviation, respectively; and A_c is the maximum acceleration calculated with the model proposed by Singh (1989) for the corresponding magnitude and a distance R_0 equal to 16 km.

The relationship presented by Boore et al. (1997), commonly used to develop engineering estimates of strong ground motion in western North America, has the following functional form:

$$\ln Y = b_1 + b_2(M-6) + b_3(M-6)^2 + b_5 \ln r + b_v \ln \frac{V_S}{V_A} \tag{2.26}$$

where

$$r = (d^2 + h^2)^{1/2} \tag{2.27}$$

and Y is the ground motion parameter (peak ground acceleration or pseudo acceleration response in g), M is the moment magnitude and d is the closest horizontal distance from the station to a point on the surface of the earth that lies directly above the rupture (in kilometers). Site conditions are represented by a continuous function of shear-wave velocity at the site, averaged to a depth of 30 m (V_S in meter/second). The coefficients b_1 to b_5, b_v and V_A were determined using a weighted two-stage regression procedure. The mean plus one sigma value of the natural logarithm of the ground motion value from equation (2.26) is $\ln Y + \sigma_{\ln Y}$, where $\sigma_{\ln Y}$ is the square root of the overall variance of the regression, given by

$$\sigma^2_{\ln Y} = \sigma_r^2 + \sigma_e^2 \tag{2.28}$$

where σ_e^2 represents the earthquake-to-earthquake component of the variability and is determined in the second stage of the regression, and σ_r^2 represents all other components of variability. The $\sigma_{\ln Y}$ value for the peak ground acceleration at 5% damping derived by the authors is equal to 0.520. They found that for peak ground acceleration $\sigma_{\ln Y}$ decreases with increasing magnitude and that most of the effect appears below magnitude 6.0. They also found that $\sigma_{\ln Y}$ decreases with increasing peak acceleration.

Grünthal and Wahlström (2001) carried out a study to assess the influence of several parameters and their uncertainties in probabilistic seismic hazard analysis. Three attenuation relations were used in their study:

$$\ln a = -2.143 + 0.751M_w - 0.815 \ln r - 1.04 \times 10^{-3} r; \qquad \sigma = 0.576 \tag{2.29}$$

$$\ln a = -3.254 + 1.045M_w - \ln r\,; \qquad \sigma = 0.437 \tag{2.30}$$

$$\ln a = -0.522 + 0.527M_w - 0.945; \qquad \sigma = 0.542 \tag{2.31}$$

where a is the horizontal peak ground acceleration, in meter per second square; M_w the moment magnitude; r the distance in kilometers; and σ is the standard deviation of the natural logarithm of a. Equation (2.29) was proposed by Ambraseys et al. (1996) based on extensive data compiled from earthquakes in Europe and Southwest Asia; equation (2.30), proposed by Sabetta and Pugliese (1996), is based on Italian data and used frequently in engineering applications; and equation (2.31), proposed by Spudich et al. (1997), is applicable to normal faulting regimes. Table 2.9 gives the domains where these equations are applicable. The authors took into account different logic tree runs with alternative magnitude sets, source models, and the main base of European earthquakes compiled in the framework of the Global Seismicity Hazard Assessment Program at the GeoForschungsZentrum Potsdam and an alternative set from the Middle Rhine area. They concluded that the three selected attenuation relations gave similar seismic hazard values, but, recommended though that efforts be made to obtain specific attenuation relations based on local regional data. They found that the increase in hazard with greater σ is small; however such effect gets slightly larger for longer mean return periods.

Table 2.9 Attenuation relations for peak ground acceleration with valid distance and magnitude ranges (reproduced from Grünthal and Wahlström, 2001)

Reference area/event type	Distance (km)	Magnitude, original	Magnitude, M_w
Ambraseys et al. (1996) Europe and adjacent areas	up to 200	$M_S = 4.0 - 7.5$	4.4 – 7.2
Sabetta and Pugliese (1996) Italy	up to 100	$M_L = 4.6 - 5.5$* $M_S = 5.5 - 6.8$	5.6 – 6.7
Spudich et al. (1997) Extensional regime earthquakes	up to 105	$M_w = 5.0 -$	5 –

* Not used.

M_w is obtained from M_S using the relation $M_w = (M_S + 1.542)/1.25$, which implicity includes the Hanks and Kanamori (19679) definition.

M_w is obtained from M_L using the relation $M_w = (M_L + 0.7222)^2 * 0.09 + 1.65$.

This conversion formulae have been established at the GeoForschungsZentrum Potsdam.

Strasser et al. (2009) presented a summary of the values of σ for peak ground acceleration and peak ground velocity that have been reported in the last 40 years, and concluded that the values of σ have remained stable, despite an increase in the number of available records and the inclusion of additional variables in the ground motion intensity models. The values of σ tend to lie between 0.15 and 0.35 in $\log_{10}$ units (0.35 to 0.80 in ln units) but in some particular cases may range as high as 0.55 in $\log_{10}$ units (1.26 in ln units).

A large number of attenuation relationships have been reported in the literature during the last five decades. Douglas (2017) has summarized most of the empirical ground motion prediction equations published between 1964 and 2016. In total, the characteristics and criteria of 442 empirical ground motion prediction equations for peak ground acceleration, and 269 for elastic response spectral ordinates are listed in his work. In addition, ground motion prediction equations derived from simulations are also listed, although its details are not given (since the work is on the empirical models). In this comprehensive report we can observe that, as new ground motion prediction models are developed (for wider ranges of magnitude, distance, site conditions, etc., than in earlier models), several new components are incorporated into them. For instance, additional predictor variables such as style of faulting, depth to the top of fault rupture, ratios of sedimentary basin amplification versus depth to basement rock, etc., and other effects on ground motion such as moderate to large magnitude scaling at close distances, rupture directivity, style of faulting (strike-slip, reverse, normal), depth to faulting (buried versus surface rupture), static stress drop (or rupture area), etc., become included. The author noted that median ground motion prediction equations show greater dispersion, demonstrating the large epistemic uncertainties involved in estimation of earthquake shaking, and recommended that this uncertainty be accounted for within seismic hazard assessments.

CHAPTER 3

POINT ESTIMATES METHODOLOGY

3.1 INTRODUCTION

It is often desirable to compute the mean and the first few statistical moments of a function of random variables, which are expressed as

$$\mu_g = \int G(\boldsymbol{X}) f(\boldsymbol{X})\, d\boldsymbol{X} \tag{3.1}$$

$$M_{kg} = \int (G(\boldsymbol{X}) - \mu_g)^k f(\boldsymbol{X})\, d\boldsymbol{X} \qquad for\ k \geq 2 \tag{3.2}$$

where $G(\boldsymbol{X})$ is a function of the random variables $\boldsymbol{X}$; $f(\boldsymbol{X})$ is the joint probability density function of $\boldsymbol{X}$; μ_g is the mean value of $G(\boldsymbol{X})$; and M_{kg} is the kth central moment of $G(\boldsymbol{X})$. Considering that $G(\boldsymbol{X})$ can be a complicated or implicit function, and that equations (3.1) and (3.2) involve in general multiple integrals, finding a solution by direct integration is almost impossible. The usual approximation is by the Taylor expansion method, which imposes excessive restrictions on the existence and continuity of the first few derivatives of the function, and requires their computation, which, in general, could be difficult to obtain. In order to overcome this problem, Rosenblueth (1975) proposed a method that uses a weighted sum of the function evaluated at a finite number of points. Considering a function of a single variable X, the estimating points x_j are chosen to satisfy the equation

$$\sum_{j=1}^{m} P_j (x_j - \mu_x)^k = M_{kx} \tag{3.3}$$

where P_j are the corresponding weights and M_{kx} is the kth central moment of X. Expressions for two-point estimate were given by Rosenblueth (1975) and Gorman (1980) derived expressions for three-point estimate as follows:

$$x_1 = \mu_x - \frac{\sigma_x}{2}(\theta - \alpha_{3x}); \qquad P_1 = \frac{1}{2}\left(\frac{1 + \frac{\alpha_{3x}}{\theta}}{\alpha_{4x} - \alpha_{3x}^2}\right) \tag{3.4a,b}$$

$$x_2 = \mu_x; \qquad P_2 = 1 - \frac{1}{\alpha_{4x} - \alpha_{3x}^2} \tag{3.5a,b}$$

$$x_3 = \mu_x + \frac{\sigma_x}{2}(\theta + \alpha_{3x}); \qquad P_3 = \frac{1}{2}\left(\frac{1 - \frac{\alpha_{3x}}{\theta}}{\alpha_{4x} - \alpha_{3x}^2}\right) \tag{3.6a,b}$$

where α_{3x} and α_{4x} are the skewness and kurtosis of X, respectively, and $\theta = (4\alpha_{4x} - 3\alpha_{3x}^2)^{\frac{1}{2}}$. The mean and kth central moment of a function $Y = Y(X)$, are then calculated by

$$\mu_y = P_1 y(x_1) + P_2 y(x_2) + P_3 y(x_3) \tag{3.7}$$

$$M_{ky} = P_1(y(x_1) - \mu_y)^k + P_2(y(x_2) - \mu_y)^k + P_3(y(x_3) - \mu_y)^k \tag{3.8}$$

This method has been applied to system reliability analysis and response uncertainty evaluation; it has been found to have the following weaknesses (Zhao & Ono, 2000):

- The accuracy in general is low especially when parameter uncertainties are large, limit state functions are highly nonlinear, or high-order moments are calculated.

- For some random variables, such as those having lognormal or exponential distributions, if the standard deviation is relatively large, estimating point x_1 in equation (3.4a,b) may lie outside of the domain of support of the probability distribution, thus making the computation impossible.

3.2 NEW POINT ESTIMATES BASED ON THE ROSENBLATT TRANSFORMATION

To overcome the limitations of the point estimate approach, Zhao and Ono (2000) developed a formulation based on the Rosenblatt transformation. A set of random variables $\boldsymbol{X}$ can be transformed into a set of independent standard normal random variables $\boldsymbol{U}$ by means of the Rosenblatt transformation as follows:

$$\begin{aligned} u_1 &= \Phi^{-1}\left[F_{X_1}(x_1)\right] \\ u_2 &= \Phi^{-1}\left[F_{X_2}(x_2|x_1)\right] \\ &\vdots \\ u_n &= \Phi^{-1}\left[F_{X_n}(x_n|x_1, x_2, \cdots, x_{n-1})\right] \end{aligned} \tag{3.9}$$

where n is the number of input variables; $F_{X_i}(x_i|x_1, x_2, \cdots, x_{i-1})$ is the cumulative distribution function of X_i conditional on $X_1 = x_1,\ X_2 = x_2, \cdots,\ X_{i-1} = x_{i-1}$; and $\Phi(\cdot)$ is the standard normal distribution function.

Thereby, using the Rosenblatt transformation, equations (3.1) and (3.2) take the form

$$\mu_g = \int G[T^{-1}(\boldsymbol{U})]\phi(\boldsymbol{U})\, d\boldsymbol{U} \tag{3.10}$$

$$M_{kg} = \int (G[T^{-1}(\boldsymbol{U})] - \mu_g)^k \phi(\boldsymbol{U})\, d\boldsymbol{U} \quad for\ k \geq 2 \tag{3.11}$$

where $T^{-1}(\boldsymbol{U}) = \boldsymbol{X}$ is the inverse Rosenblatt transformation and $\phi(\cdot)$ is the standard normal probability density function. Consider the case of a function of a single random variable X. According to Rosenblatt transformation, $u = \Phi^{-1}[F_X(x)]$; the moments or the standard normal variable U, can be expressed as

$$\int u^k \exp(-\frac{1}{2}u^2)\, du = \sqrt{2\pi}\sum_{j=1}^{m} P_j u_j^k \tag{3.12}$$

given that the left hand side is a Hermite integration with weight function $\phi(u) = \exp\left(-\frac{u^2}{2}\right)$. Therefore, the estimating points u_j and weights P_j are readily defined in the right hand side of (3.12) for given m. Table 3.1 gives the estimating points and weights for m=5 and 7.

Table 3.1 Estimating points u_j and weights P_j for m=5 and 7

m	u_0	$u_{1+} = -u_{1-}$	$u_{2+} = -u_{2-}$	$u_{3+} = -u_{3-}$	P_0	P_1	P_2	P_3
5-point estimate	0	1.3556262	2.8569700	-	8/15	0.2220759	0.0112574	-
7-point estimate	0	1.1544054	2.3667594	3.7504397	16/35	0.2401233	0.0307571	0.000548269

Now let, $x_j = T^{-1}(u_j) = F_X^{-1}[\Phi(u_j)]$, $j = 1, \dots, m$; the mean and variance of function $Y(X)$ can be calculated as

$$\mu_Y = \sum_{j=1}^{m} P_j Y(x_j) \tag{3.13}$$

$$\sigma_Y^2 = \sum_{j=1}^{m} P_j \big(Y(x_j) - \mu_Y\big)^2 \tag{3.14}$$

Note that the general expression for the function $Y(x) = Y[T^{-1}(u)]$ is not necessary in equations (3.13) and (3.14): the Rosenblatt transformation is only required at the estimating points x_j. This method has several advantages over the classical point estimate methods: (1) the number of estimating points can be increased easily, if necessary, since they are independent of the random variables in the original space; (2) the use of high-order moments of the random variables is not required; (3) estimating points do not fall outside the domain of the random variables; and (4) accurate estimates of the first two statistical moments can be obtained using few (e.g. five or seven) estimation points.

This procedure can be extended straightforwardly to functions $G(\boldsymbol{X})$ of a random vector $\boldsymbol{X} = (X_1, X_2, \dots, X_n)$. In this case, the multivariate probability density is concentrated at m^n points in the hyperspace defined by the n random variables. However, if n is a very large number computations may become intensive. Thus, Zhao and Ono (2000, 2001) proposed to use the following approximation for function $G(\boldsymbol{X})$:

$$G'(\boldsymbol{X}) = \sum_{i=1}^{n} \big(G_i - G_\mu\big) + G_\mu \tag{3.15}$$

where

$$G_\mu = G(\boldsymbol{\mu}) \tag{3.16}$$

$$G_i = G[T^{-1}(\boldsymbol{U}_i)] \tag{3.17}$$

In equations (3.16) and (3.17), $\boldsymbol{\mu}$ is the mean vector of $\boldsymbol{X}$; $\boldsymbol{U}_i$ means only U_i is treated as random variable, with all of the other variables set equal to their mean values transformed into standard normal space, and G_i is a function of only U_i. Since $\boldsymbol{U} = T(\boldsymbol{X})$ are mutually independent and G_i, $i = 1, 2, \dots, n$, are also statistically independent, then from equation (3.15),

$$\mu_G = \sum_{i=1}^{n} (\mu_i - G_\mu) + G_\mu \tag{3.18}$$

$$\sigma_G^2 = \sum_{i=1}^{n} \sigma_i^2 \tag{3.19}$$

where μ_i and σ_i^2 are the first two moments of G_i, which can be obtained using the point estimate formulation for functions of a single variable.

3.3 POINT ESTIMATES METHODOLOGY FOR PSHA

The extensive literature review reported in Chapter 2 indicated that there is limited research concerning the assessment of the effect of parameter uncertainty on PSHA; nevertheless, previous studies have identified the parameters that have a greater impact on the magnitude distribution and the ground motion prediction models that are used in PSHA. Taking into account the statistical characteristics of the uncertain parameters found in the literature review, and the point estimate central-moment formulas based on the Rosenblatt transformation, the following formulation is developed here in order to apply point estimation for assessing the impact of parameter uncertainty on probabilistic seismic hazard analysis.

3.3.1 Uncertainty in only one parameter

When uncertainty in only one parameter is taken into account, the analytical solution, for any of the three cases of PSHA, is treated as a function of a single random variable. For this single-variable function, the mean value and the variance can be computed from equations (3.13) and (3.14), respectively. Consider, for instance, the case of uncertainty in parameter β. The intensity exceedance rate $v(a)$ is then expressed as $v(\beta|a)$, for which the mean value and the variance are

$$E[v(\beta|a)] = \mu_v = \sum_{j=1}^{m} P_j v\left[T^{-1}(u_j|a)\right] \tag{3.20}$$

$$Var[v(\beta|a)] = \sigma_v^2 = \sum_{j=1}^{m} P_j \left(v\left[T^{-1}(u_j|a)\right] - \mu_v\right)^2 \tag{3.21}$$

where u_j and P_j are the estimating points and corresponding weights. From the definition of the Rosenblatt transformation, we have

$$T^{-1}(u_j) = F_\beta^{-1}\left(\Phi(u_j)\right) = \beta_j \tag{3.22}$$

where $F_\beta(\cdot)$ is the distribution function of β. Hence, rewriting equations (3.20) and (3.21), one obtains

$$E[v(\beta|a)] = \mu_v(a) = \sum_{j=1}^{m} P_j v(\beta_j|a) \tag{3.23}$$

$$Var[v(\beta|a)] = \sigma_v^2(a) = \sum_{j=1}^{m} P_j\left(v\left(\beta_j|a\right) - \mu_v(a)\right)^2 \tag{3.24}$$

This procedure is employed likewise when uncertainty in parameter σ is considered only.

3.3.2 Uncertainty in two parameters

When both parameters are uncertain, the analytical solutions for cases (2) and (3) of PSHA become functions of two random variables. Let $G(X_1,\ X_2)$ be a function of two random variables. The point estimate first-moment formula based on the Rosenblatt transformation given in equation (3.10) can be expressed as

$$\mu_G = \int_{u_2}\int_{u_1} G[T^{-1}(u_1, u_2)]\phi(u_1, u_2)\, du_1\, du_2 \tag{3.25}$$

Given that $U_1$and U_2 are statistically independent,

$$\mu_G = \int_{u_2}\int_{u_1} G[T^{-1}(u_1, u_2)]\phi(u_1)\phi(u_2)\, du_1\, du_2 \tag{3.26}$$

and rearranging terms

$$\mu_G = \int_{u_2} \phi(u_2) \int_{u_1} G[T^{-1}(u_1, u_2)]\phi(u_1)\, du_1\, du_2 \tag{3.27}$$

Let $h(u_2)$ be a function such that $h(u_2) = \int_{u_1} G[T^{-1}(u_1, u_2)]\phi(u_1)\, du_1$; substituting in equation (3.27) we have:

$$\mu_G = \int_{u_2} h(u_2)\phi(u_2)\, du_2 \tag{3.28}$$

Equation (3.28) represents the case of a single random variable function, and thus from equation (3.13),

$$\mu_G = \sum_{j=1}^{m} P_j h\left(u_{2_j}\right) \tag{3.29}$$

Given that $h(u_2)$ can be treated as a function of only one random variable as well, then

$$h\left(u_{2_j}\right) = \int_{u_1} G\left[T^{-1}\left(u_1, u_{2_j}\right)\right]\phi(u_1)\, du_1 = \sum_{k=1}^{m} P_k G\left[T^{-1}\left(u_{1_k}, u_{2_j}\right)\right] \tag{3.30}$$

Replacing equation (3.30) into equation (3.29) yields

$$\mu_G = \sum_{j=1}^{m} P_j \sum_{k=1}^{m} P_k G\left[T^{-1}\left(u_{1_k}, u_{2_j}\right)\right] \tag{3.31}$$

The corresponding procedure for obtaining the variance of the function is similar to the one derived above, yielding the expression

$$\sigma_G^2 = \sum_{j=1}^{m} P_j \sum_{k=1}^{m} P_k \left(G\left[T^{-1}\left(u_{1_k}, u_{2_j}\right)\right] - \mu_g\right)^2 \tag{3.32}$$

When both parameters β and σ are considered uncertain in the PSHA, the intensity exceedance rate is expressed as $v(a) = v(\beta, \sigma|a)$. From equations (3.31) and (3.32), the mean and variance of the intensity exceedance rate can be estimated as

$$E[v(\beta, \sigma|a)] = \mu_v(a) = \sum_{j=1}^{m} P_j \sum_{k=1}^{m} P_k v\left(\beta_j, \sigma_k|a\right) \tag{3.33}$$

$$Var[v(\beta, \sigma|a)] = \sigma_v^2(a) = \sum_{j=1}^{m} P_j \sum_{k=1}^{m} P_k \left(v(\beta_j, \sigma_k|a) - \mu_v(a)\right)^2 \tag{3.34}$$

where from the Rosenblatt transformation,

$$\begin{aligned} \beta_j &= T^{-1}\left(u_{1_j}\right) = F_\beta^{-1}\left(\Phi\left(u_j\right)\right) \\ \sigma_k &= T^{-1}\left(u_{2_k}\right) = F_{\sigma|\beta}^{-1}\left(\Phi\left(u_k|\beta_j\right)\right) \end{aligned} \tag{3.35}$$

and $F_{\sigma|\beta}(\cdot)$ is the conditional distribution function of σ given β. If parameters β and σ are statistically independent, then

$$\begin{aligned} \beta_j &= T^{-1}\left(u_{1_j}\right) = F_\beta^{-1}\left(\Phi\left(u_j\right)\right) \\ \sigma_k &= T^{-1}\left(u_{2_k}\right) = F_\sigma^{-1}\left(\Phi(u_k)\right) \end{aligned} \tag{3.36}$$

where $F_\sigma(\cdot)$ is the distribution function of σ.

CHAPTER 4
CASE STUDIES

4.1 INTRODUCTION

Case studies were carried to assess the effect of uncertainty in parameters β and σ on the analytical solutions for the PGA exceedance rates described in section 2.2 using the point estimate method proposed in section 3.3. The accuracy of the method was validated based on Monte Carlo simulations. Results when no parameter uncertainty is considered are presented as well; in this case all of the involved parameters are considered to be deterministic. The statistics for parameters β and σ were selected based on the literature review in section 2.3. The set of seismicity and ground motion parameters shown in Table 4.1 and Table 4.2, as proposed by Ordaz (2004), are considered for the case studies.

Table 4.1 Seismicity parameters

	Parameter		
	λ_0	M_0	M_U
Value	1/year	4	8

Table 4.2 Attenuation parameters

	Parameter			
	a_1	a_2	a_3	a_4
Value	4.0530	0.6910	-1.0000	-0.0071

4.2 CASE (1): POINT-SOURCE, DETERMINISTIC MEDIAN ATTENUATION RELATION

This case study is the simplest since for a deterministic median attenuation relation $\sigma = 0$ and only uncertainty in β is considered. The analytical solution given in equation (2.5) becomes a function of only one random variable, $v(\beta|a)$, and the first two central moments were calculated from equations (3.23) and (3.24). Results for the intensity exceedance rates were computed for a point source located at a distance $R = 30$ km from the site and assuming that parameter β follows a lognormal probability distribution.

The mean annual exceedance rate was estimated considering a mean value of β equal to 2.0 and coefficients of variation equal to 5%, 10% and 20%. Results are shown in Figure 4.1. The overall effect of including parameter uncertainty is to increase the mean exceedance rate for a given PGA. For this case study it is seen that there is little parameter uncertainty influence for coefficients of variation less than 10%. In fact, it is observed that for 5% coefficient of variation results are practically equal to the case where parameter uncertainty is not taken into account. The effect of parameter uncertainty becomes more significant for 20% coefficient of variation. The variation of the mean annual exceedance rate, μ_v, and of the mean plus/minus one standard deviation, $\mu_v \pm \sigma_v$, versus the PGA are shown in Figure 4.2. It is seen that the effect of parameter uncertainty increases greatly with PGA. For some return periods of interest, PGA values from Figure 4.2 are listed in Table 4.3, including the case where parameter

uncertainty is not taken into account. Take for instance a 500-year event: the PGA from seismic hazard analysis is equal to 200 Gal, however, when parameter uncertainty is considered, the mean exceedance rate yields a PGA equal to 235 Gal and from $\mu_\nu \pm \sigma_\nu$ a value of 289 Gal is obtained. These represent increments of the PGA of about 15% and 45%, respectively, if parameter uncertainty is accounted for.

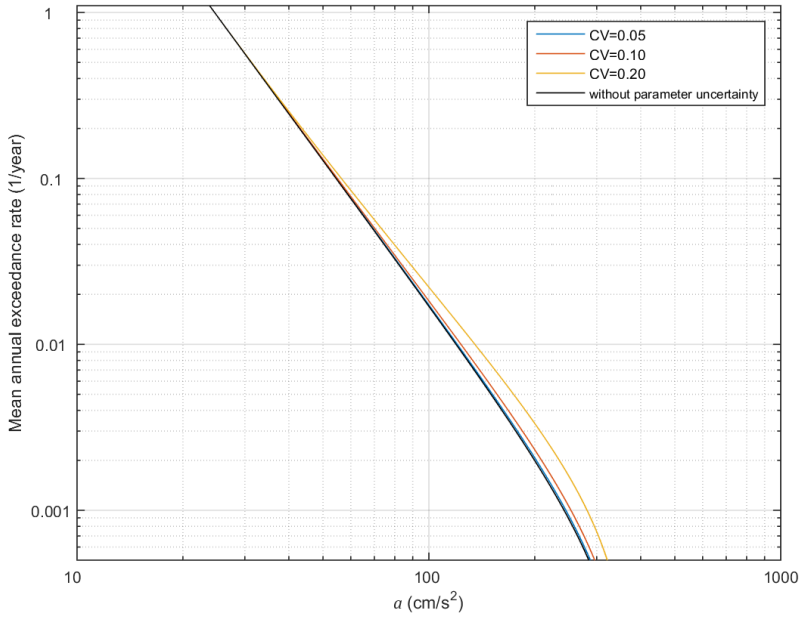

Figure 4.1 Case (1): Influence of the uncertainty in parameter β on the mean annual exceedance rate

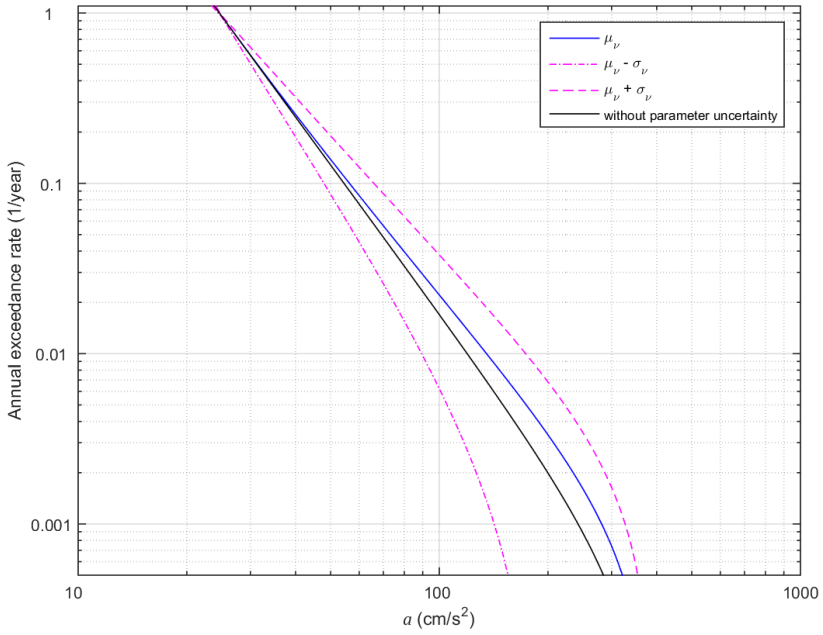

Figure 4.2 Case (1): Uncertainty in the annual exceedance rate due to uncertainty in parameter β; $E[\beta]$=2.0 and CV=0.20

Table 4.3 Case (1): Peak ground acceleration values from μ_v and $\mu_v \pm \sigma_v$ for some return periods; $E[\beta]$=2.0 and CV=0.20

Annual exceedance rate (1/year)	Return period (year)	Peak ground acceleration (Gal)			
		Without parameter uncertainty	Uncertainty in β		
			μ_v	$\mu_v - \sigma_v$	$\mu_v + \sigma_v$
0.020	50	95	104	75	131
0.010	100	119	135	89	173
0.002	500	200	235	127	289
0.001	1000	242	282	142	327

The accuracy of the point estimates was examined in comparison to Monte Carlo estimates using ensembles of 50,000 simulations. Results for estimates of the mean and variance of the exceedance rate are shown in Figure 4.3. It can be appreciated that mean estimates differ by less than 1.5% and variance estimates by 3%. These results indicate that the point estimate method was able to assess the mean and variance of the exceedance rate with great accuracy.

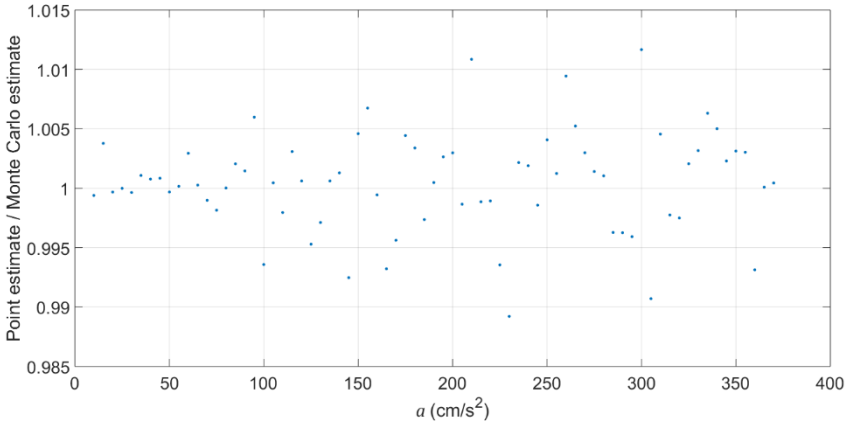

a) Mean

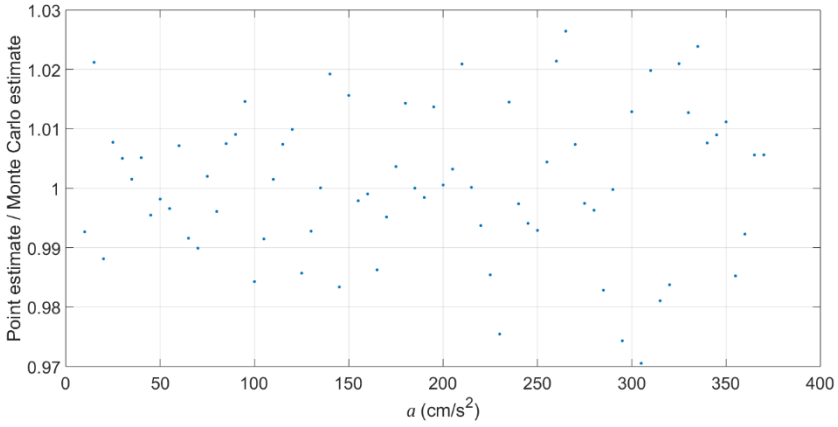

b) Variance

Figure 4.3 Case (1): Comparison between the mean and variance point estimates of the annual exceedance rate with 50,000 Monte Carlo simulations estimates; CV=0.20

The effect of the parameter uncertainty on the exceedance rate was also analyzed for mean values of β equal to 1.5 and 2.5, i.e., the lowest and the highest values reported in the literature. It can be observed from Figure 4.4 that assigning a higher mean value to the uncertain parameter decreases the expected number of seismic events, per year, that will exceed a certain intensity a. In general, it is observed that the shape of the curves representing the mean, μ_ν, and the mean plus/minus one standard deviation, $\mu_\nu \pm \sigma_\nu$, is due to the cut-off limits imposed by the modified Gutenberg-Richter model, implying that when the PGA value is far from those limits the uncertainty in the annual exceedance rates is higher.

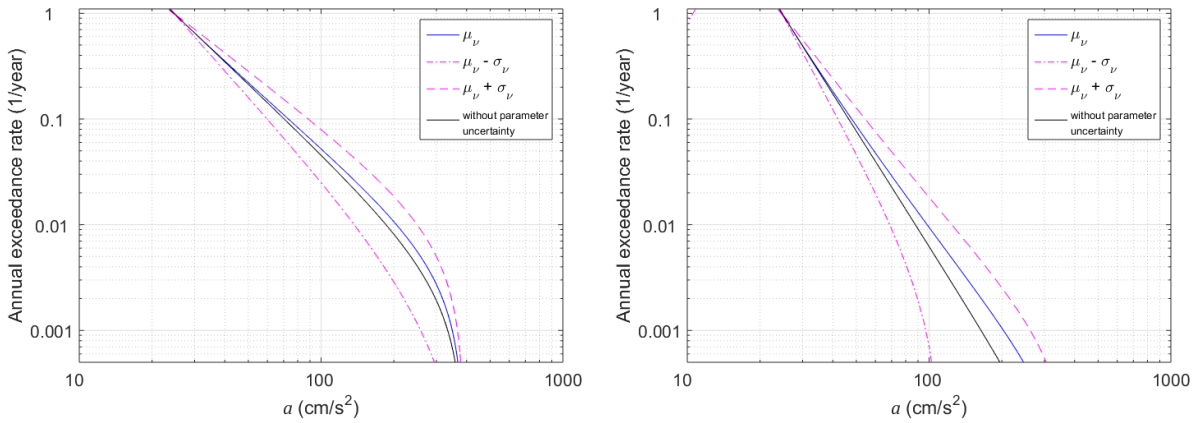

a) $E[\beta] = 1.5$ b) $E[\beta] = 2.5$

Figure 4.4 Case (1): Uncertainty in the annual exceedance rate due to uncertainty in parameter β; $\sigma = 0.5$ and CV=0.20

4.3 CASE (2): POINT-SOURCE, PROBABILISTIC ATTENUATION RELATION

The analysis is performed using the analytical solution given in equation (2.7) for the exceedance rate of PGA, assuming parameters β and σ to follow a lognormal probability distribution, with mean values equal to 2.0 and 0.5, respectively. Values of coefficient of variation equal to 10%, 20% and 40% were considered for β and σ to include various degrees of uncertainty in these parameters. When only one of these is considered uncertain, the mean and variance of the PGA exceedance rate were computed based on equations (3.23) and (3.24); when both parameters are uncertain, the mean and variance were calculated using equations (3.33), (3.34) and (3.36) assuming statistical independence. A point source located at a distance $R = 30$ km from the site is considered.

Figure 4.5a shows the variation of the mean exceedance rate of PGA with the coefficient of variation of β, CV_β. For return periods greater than 10 years, the mean exceedance rate is greater than the deterministic exceedance rate computed without accounting for parameter uncertainty. The effect of including parameter uncertainty is thus to obtain greater values of PGA associated with a given nominal exceedance rate or return period. It can be observed that for lower levels of uncertainty, such as CV_β=10%, the results are very similar to those where parameter uncertainty is not considered. For higher degrees of uncertainty, say CV_β values equal to 20% and 40%, the differences in the estimated exceedance rate become more noticeable. Similar trends are shown in Figure 4.5b for the mean exceedance rate of PGA when uncertainty in parameter σ is taken into account. However, in this case higher uncertainties in σ are required, say CV_σ=40%, for the effect of parameter uncertainty to become noticeable as compared to the deterministic case where it is not included.

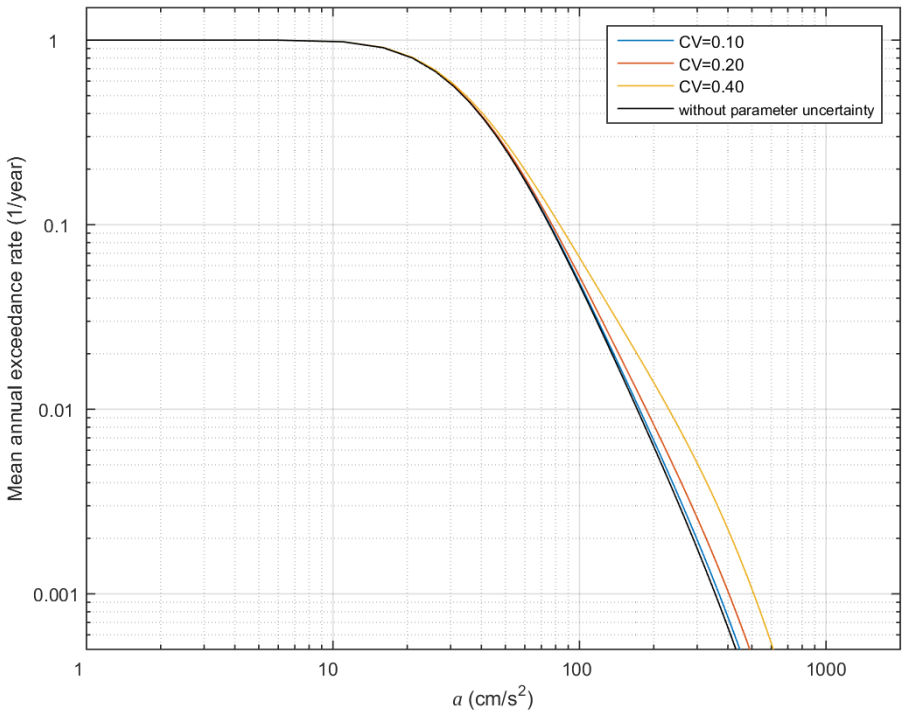

a) Uncertainty in parameter β

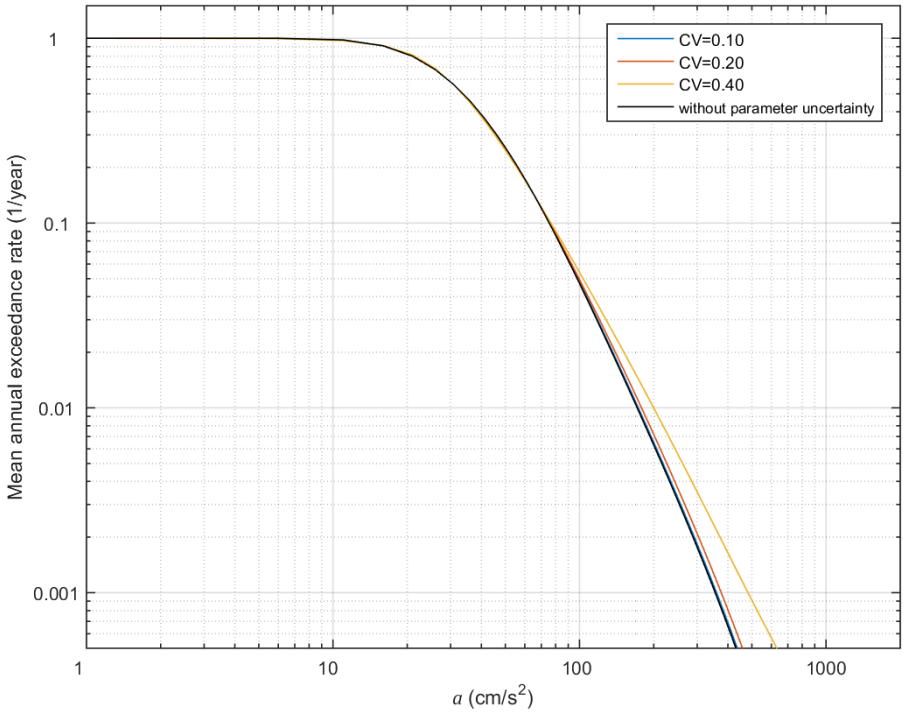

b) Uncertainty in parameter σ

Figure 4.5 Case (2): Influence of parameter uncertainty on the mean annual exceedance rate

The effect of considering uncertainty in both parameters β and σ is shown in Figure 4.6 for 20% coefficients of variation. Results for the case without parameter uncertainty are also shown. It is observed that for a given mean annual exceedance rate, greater PGA values are obtained when uncertainty in both parameters is taken into account. Recalling results in Figure 4.5, it is clear in Figure 4.6 that uncertainty in parameter β has a greater effect on the mean exceedance rate than that in σ. Table 4.4 summarizes PGA values for some return periods. For instance, for a 500-year event, the PGA value computed without considering parameter uncertainty increases about 5% and 13% when uncertainty only in parameter σ or β is considered, respectively. When uncertainty about both parameters is taken into account, the PGA value increases about 18%. Such an effect becomes less or greater for shorter or longer return periods.

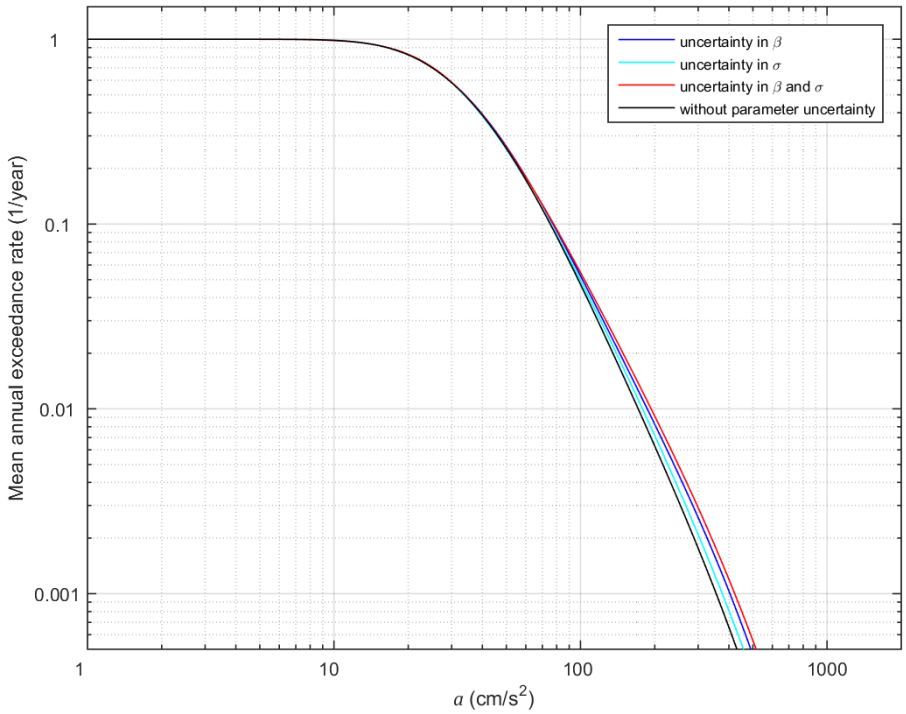

Figure 4.6 Case (2): Effect of parameter uncertainty on the mean annual exceedance rate; $E[\beta] = 2.0$, $E[\sigma] = 0.5$ and CV=0.20

Table 4.4 Case (2): Peak ground acceleration values from μ_v for some return periods; $E[\beta] = 2.0$, $E[\sigma] = 0.5$ and CV=0.20

Mean annual exceedance rate (1/year)	Return Period (year)	Peak ground acceleration (Gal)			
		Without parameter uncertainty	Uncertainty in β	Uncertainty in σ	Uncertainty in β and σ
			μ_v	μ_v	μ_v
0.020	50	135	144	140	149
0.010	100	171	186	179	193
0.002	500	289	326	304	340
0.001	1000	355	404	376	422

Results obtained for the mean exceedance rate, μ_v, and the mean plus/minus one standard deviation, $\mu_v \pm \sigma_v$, are shown in Figure 4.7. As seen, parameter uncertainty has a greater effect on the uncertainty of the annual exceedance rates when both parameters are taken to be uncertain. When uncertainty in only one parameter is accounted for, that of parameter β is more noticeable. Table 4.5 lists PGA values, for some return periods; e.g., for a 500-year seismic event, the traditional PSHA without including parameter uncertainty yields a PGA value equal to 289 Gal; the PGA values for $\mu_v + \sigma_v$, are equal to 364, 402 and 436 Gals when uncertainty is considered in σ only, β only, and in both of them, which represent increments of about 25%, 40% and 50%, respectively. In the case of a nominal 100-year return period, the corresponding effect of accounting for parameter uncertainty is about 22%, 35% and 43%, respectively.

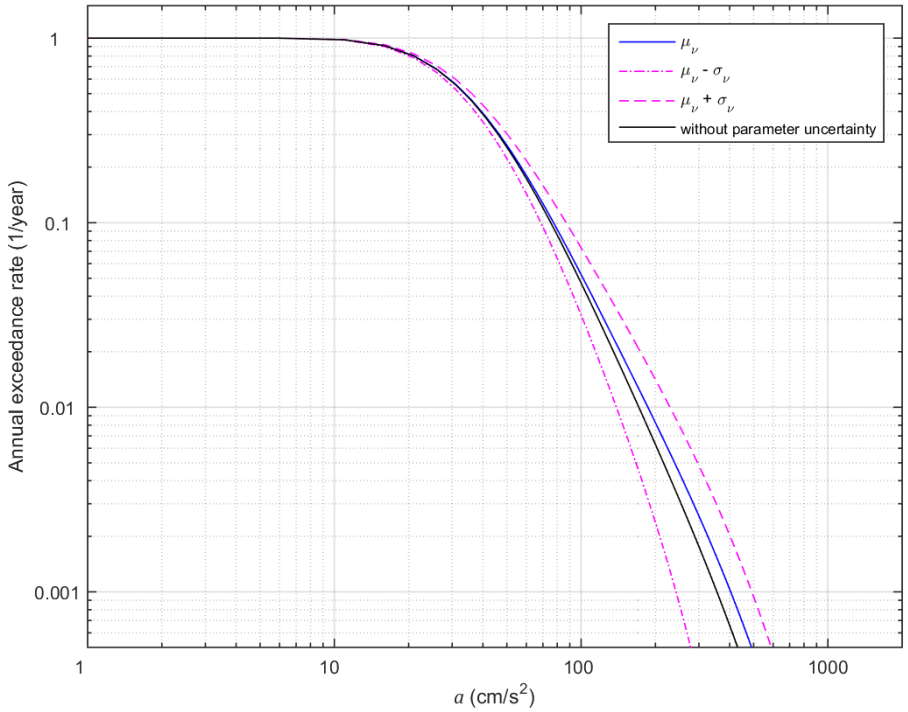

a) Uncertainty in parameter β

Figure 4.7 Case (2): Uncertainty in the annual exceedance rate due to parameter uncertainty; $E[\beta] = 2.0$, $E[\sigma] = 0.5$ and CV=0.20

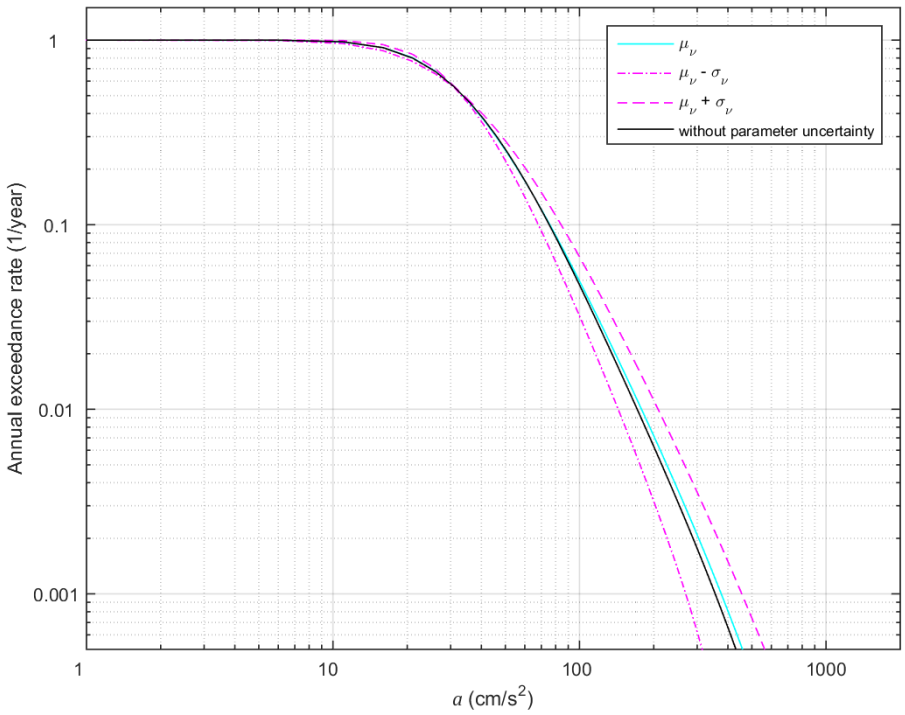

b) Uncertainty in parameter σ

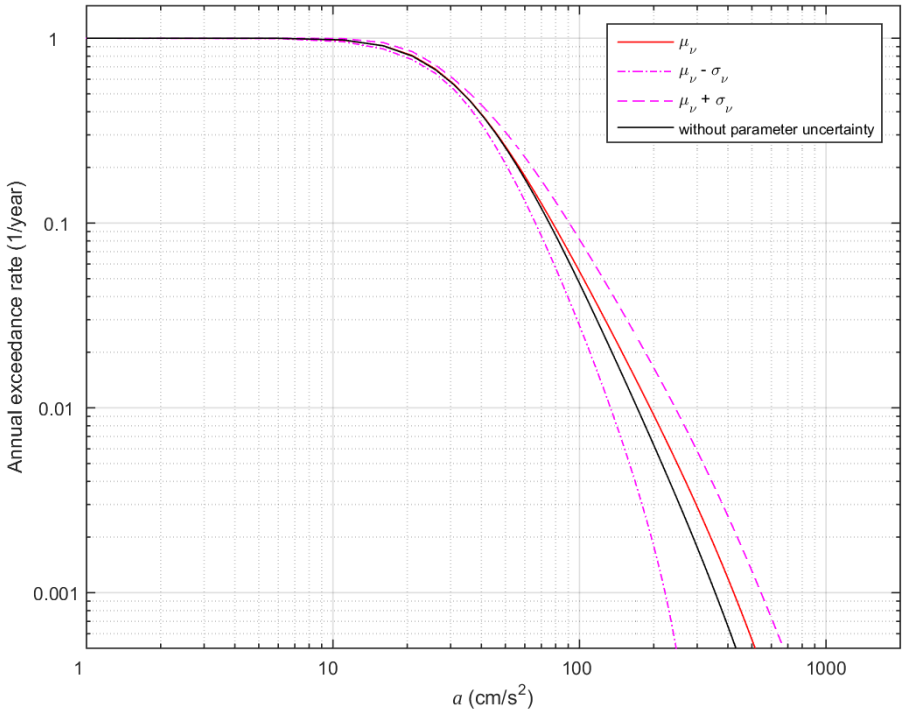

c) Both parameters considered uncertain

Figure 4.7 – Continued

Table 4.5 Case (2): Peak ground acceleration values from $\mu_v \pm \sigma_v$ for some return periods; $E[\beta] = 2.0$, $E[\sigma] = 0.5$ and CV=0.20

Annual exceedance rate (1/year)	Return period (year)	Peak ground acceleration (Gal)						
		Without parameter uncertainty	Uncertainty in β		Uncertainty in σ		Uncertainty in β and σ	
			$\mu_v - \sigma_v$	$\mu_v + \sigma_v$	$\mu_v - \sigma_v$	$\mu_v + \sigma_v$	$\mu_v - \sigma_v$	$\mu_v + \sigma_v$
0.020	50	135	115	174	116	161	110	185
0.010	100	171	139	229	144	208	134	244
0.002	500	289	208	402	227	364	196	436
0.001	1000	355	242	492	270	455	222	545

The accuracy of the point estimate method using $m = 5$ was assessed by means of comparisons to Monte Carlo estimates using 250,000 simulations. Results for the mean and variance of the exceedance rate are shown in Figure 4.8 and Figure 4.9, respectively, for the range of PGA values given in Table 4.4 and Table 4.5. Estimates of the mean differ by less than 0.4%, when parameter β is considered to be uncertain, 0.5% when σ, and 0.6% when both parameters are taken to be uncertain. In the case of the variance, estimates differ by less than 1.5%, 5% and 2.5% considering the uncertainty in β, in σ, and in both parameters. Hence, the point estimate method yields pretty accurate results for both the mean and the variance of the exceedance rate.

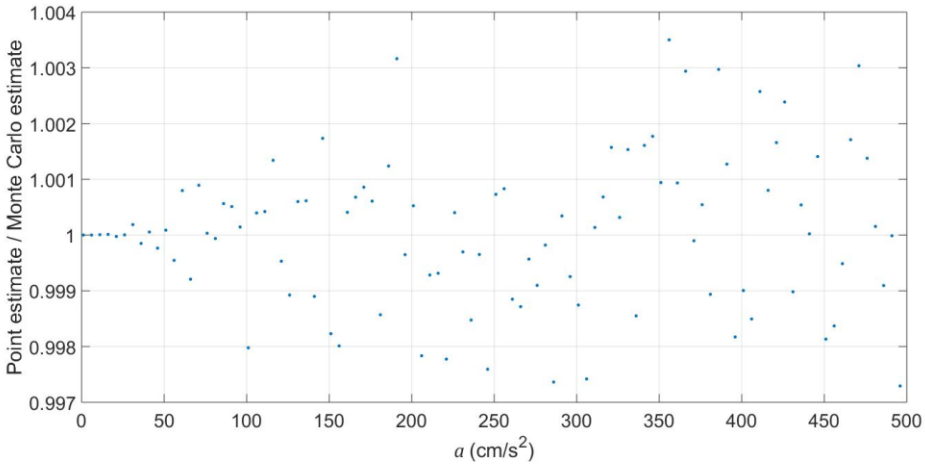

a) Uncertainty in parameter β

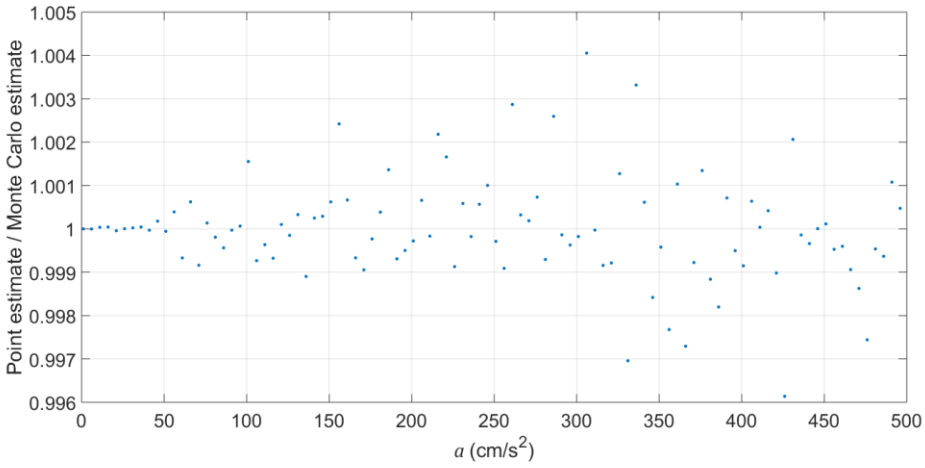

b) Uncertainty in parameter σ

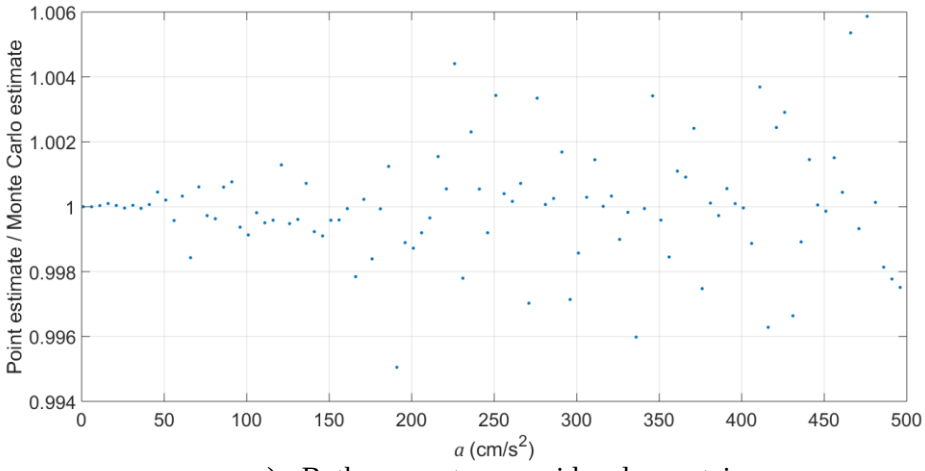

c) Both parameters considered uncertain

Figure 4.8 Case (2): Comparison between the mean point estimates of the annual exceedance rates with estimates from 250,000 Monte Carlo simulations; CV=0.20

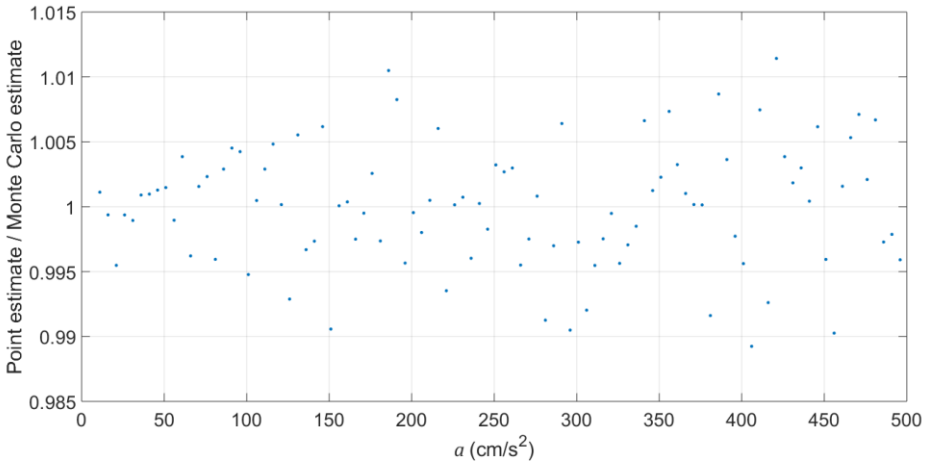

a) Uncertainty in parameter β

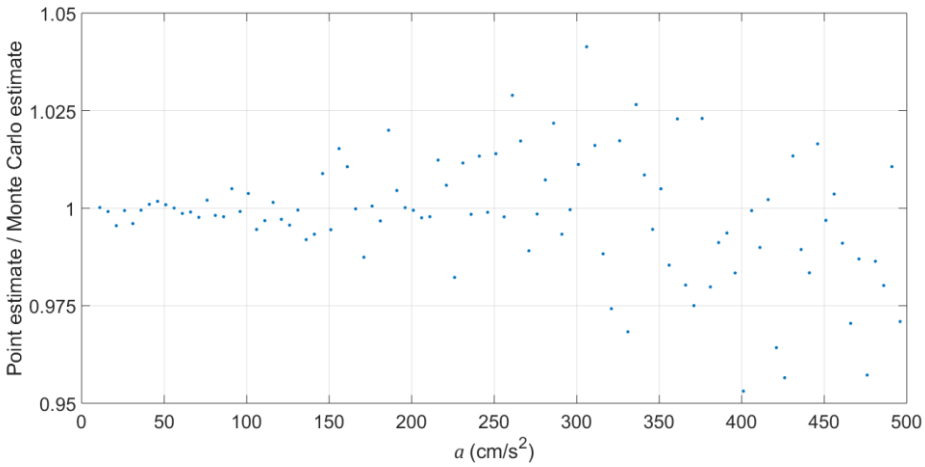

b) Uncertainty in parameter σ

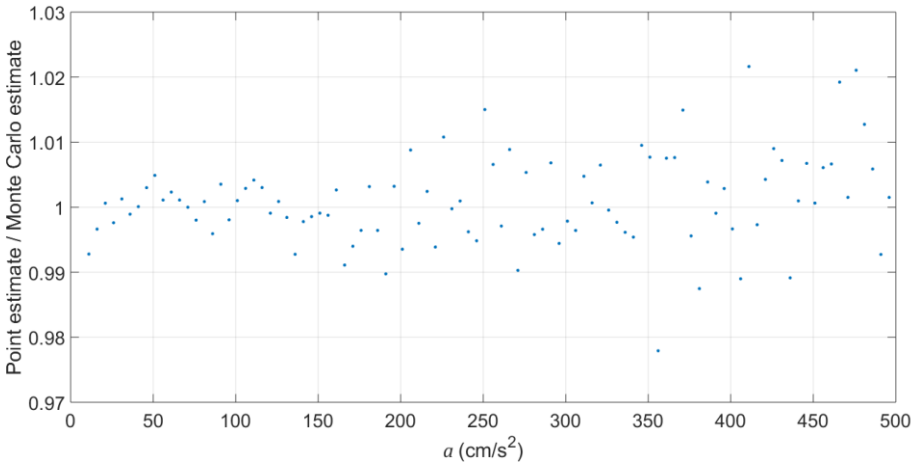

c) Both parameters considered uncertain

Figure 4.9 Case (2): Comparison between the variance point estimates of the annual exceedance rates with estimates from 250,000 Monte Carlo simulations; CV=0.20

In order to examine the effects of greater parameter uncertainty, results were obtained using coefficients of variation equal to 40% for β and σ. Results for the mean exceedance rate, μ_v, and the mean plus/minus one standard deviation, $\mu_v \pm \sigma_v$, are shown in Figure 4.10. As for 20% coefficient of variation, the overall trend of a greater mean and a larger variance of the exceedance rate can be observed when uncertainty in both parameters is taken into account. PGA values for some return periods are listed in Table 4.6. As seen, the effect of parameter uncertainty is considerable. Compared to results without dealing with parameter uncertainty, PGA values increase by about 50% and 70% for nominal 100 and 500-year return periods when uncertainty in both parameters is accounted for. Table 4.7 shows the range of PGA values for annual exceedance rates in the interval of one plus/minus standard deviation around the mean. It can be appreciated that for 40% coefficients of variation the effect on the PGA values is significant and clearly higher than for the previous case of 20%. As expected, there is also a greater effect when both parameters are taken to be uncertain. However, unlike the previous case, the effect of parameter σ on $\mu_v \pm \sigma_v$ now becomes greater than that of β for the longer return periods. For instance, for 500-year return period, PGA values for $\mu_v + \sigma_v$ increase by about 90% when parameter β is the only one uncertain, 170% when the uncertain parameter is σ, and 230% when both parameters are uncertain. In the case of a nominal 100-year return period, the corresponding effect of accounting for parameter uncertainty amounts an increase of about 90%, 85%, and 135%, respectively.

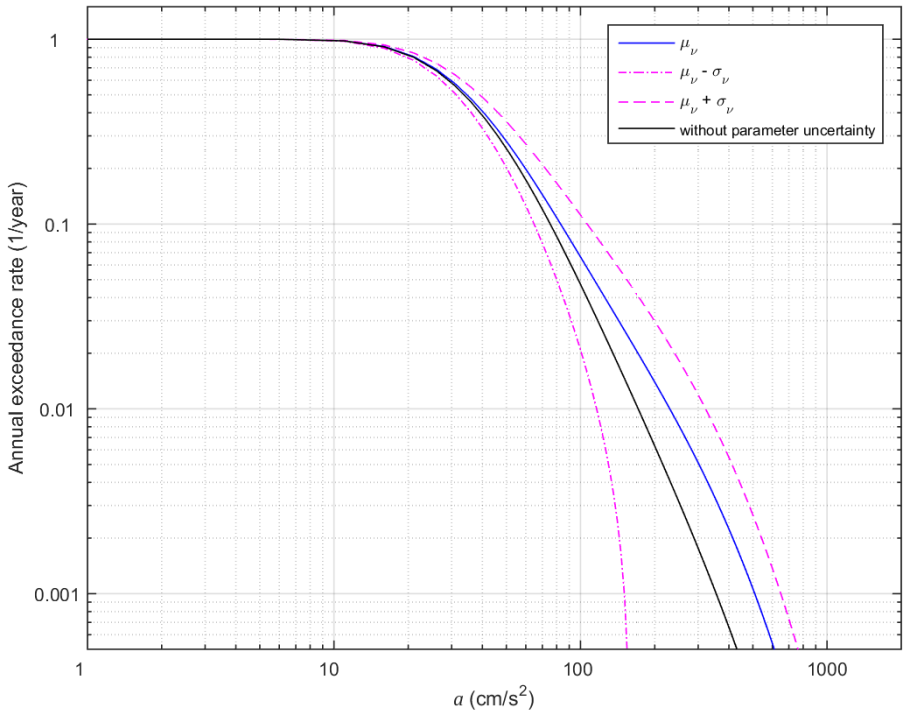

a) Uncertainty in parameter β

Figure 4.10 Case (2): Uncertainty in the annual exceedance rates due to parameter uncertainty; $E[\beta] = 2.0$, $E[\sigma] = 0.5$ and CV=0.40

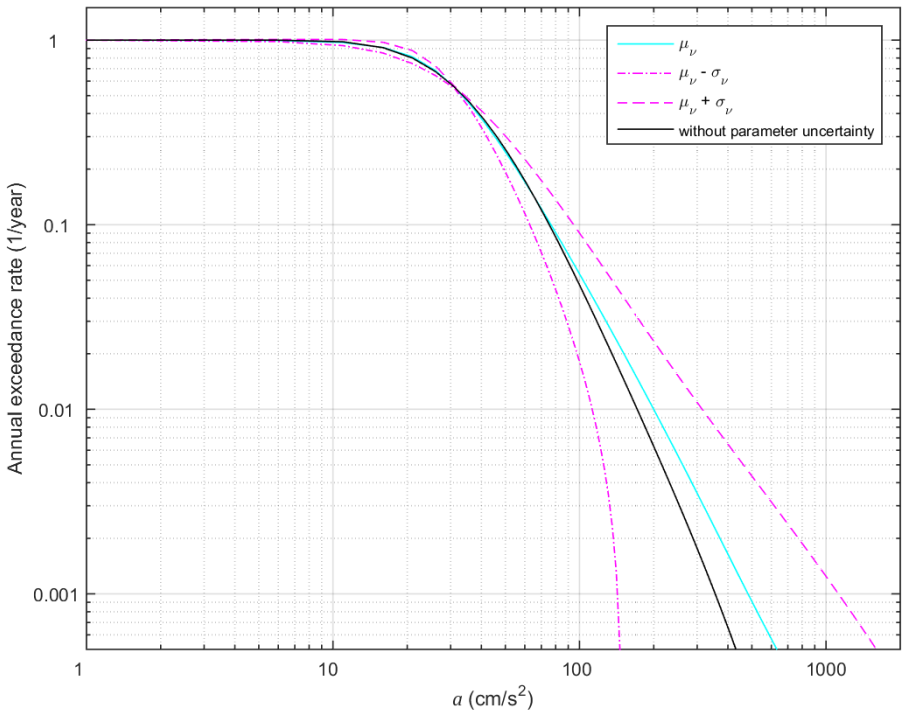

b) Uncertainty in parameter σ

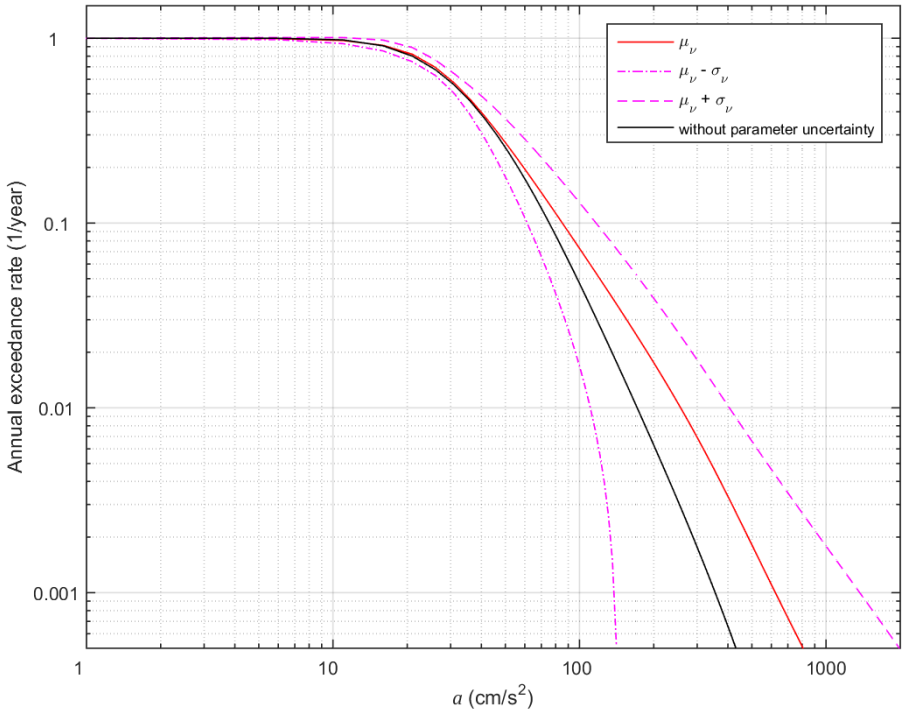

c) Both parameters considered uncertain

Figure 4.10 – Continued

Table 4.6 Case (2): Peak ground acceleration values from μ_v for some return periods; $E[\beta] = 2.0$, $E[\sigma] = 0.5$ and CV=0.40

Mean annual exceedance rate (1/year)	Return period (year)	Peak ground acceleration (Gal)			
		Without parameter uncertainty	Uncertainty in β	Uncertainty in σ	Uncertainty in β and σ
			μ_v	μ_v	μ_v
0.020	50	135	171	151	188
0.010	100	171	230	200	257
0.002	500	289	414	371	483
0.001	1000	355	509	482	623

Table 4.7 Case (2): Peak ground acceleration values from $\mu_v \pm \sigma_v$ for some return periods; $E[\beta] = 2.0$, $E[\sigma] = 0.5$ and CV=0.40

Annual exceedance rate (1/year)	Return period (year)	Peak acceleration (Gal)						
		Without parameter uncertainty	Uncertainty in β		Uncertainty in σ		Uncertainty in β and σ	
			$\mu_v - \sigma_v$	$\mu_v + \sigma_v$	$\mu_v - \sigma_v$	$\mu_v + \sigma_v$	$\mu_v - \sigma_v$	$\mu_v + \sigma_v$
0.020	50	135	101	241	98	217	96	286
0.010	100	171	116	321	113	314	111	405
0.002	500	289	144	543	137	772	134	941
0.001	1000	355	151	649	143	1123	138	1370

A comparison between point estimates of the mean and variance of the annual exceedance rate and estimates from 250,000 Monte Carlo simulations is shown in Figure 4.11 and Figure 4.12, respectively, for the range of PGA values associated to the return periods in Table 4.6 and Table 4.7. Mean estimates differ by less than 3%. In the case of the variance estimates differ by less than 2.5%, 20% and 10% if uncertainty is considered in parameter β, in parameter σ, and in both parameters, respectively. The largest difference in the variance estimates observed in Figure 4.12b is about 19% for a PGA equal to 391 Gal. Because of the large uncertainty being considered in parameter σ and that a second-order moment is being estimated, it may be that the Monte Carlo estimate based on 250,000 simulations is not accurate enough to assess the performance of the point estimate method. To examine this argument, an analysis was performed where the variance estimate for PGA=391 Gal was computed varying the size of the simulated ensembles from 5×10^4 to 5×10^6. Monte Carlo estimates were computed for six different ensembles generated for each size. Figure 4.13 shows a comparison of the variance point estimates and those based on Monte Carlo simulations. The results show that as the size of the simulated ensembles increases the Monte Carlo estimate approaches a stable value. Considering that for such a large ensemble size as 5×10^6, the variance estimate from Monte Carlo is accurate enough, it is now seen that the error in the point estimate method is about 9%. In view of this analysis, we can expect that if the same procedure was performed for a different PGA value within the range covered in Figure 4.12b, point estimates and Monte Carlo estimates would differ by about 9% or even less. Compared to 20% coefficients of variation for β and σ, the point estimate method in this case is still pretty accurate for estimating the mean of the exceedance rate, but it is now less accurate for the estimation of the variance.

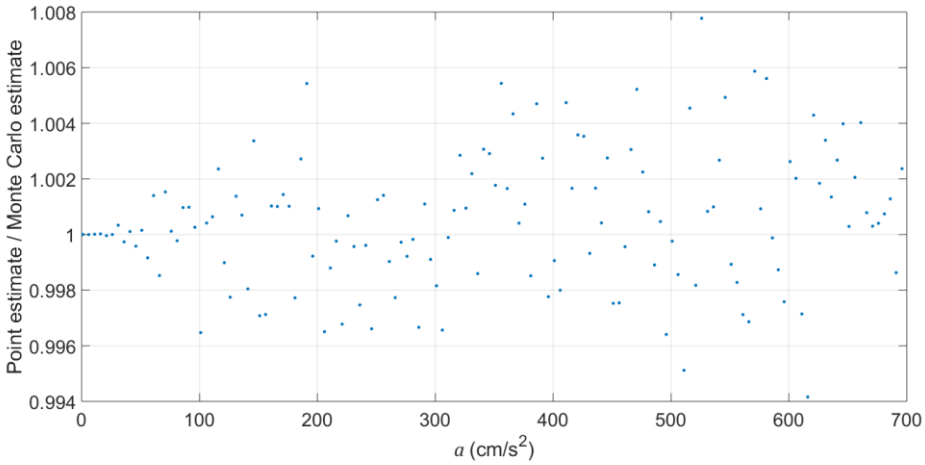

a) Uncertainty in parameter β

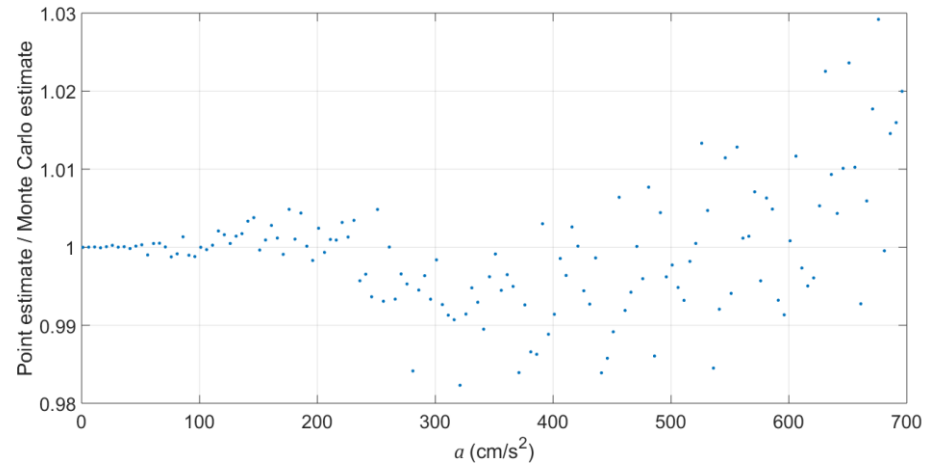

b) Uncertainty in parameter σ

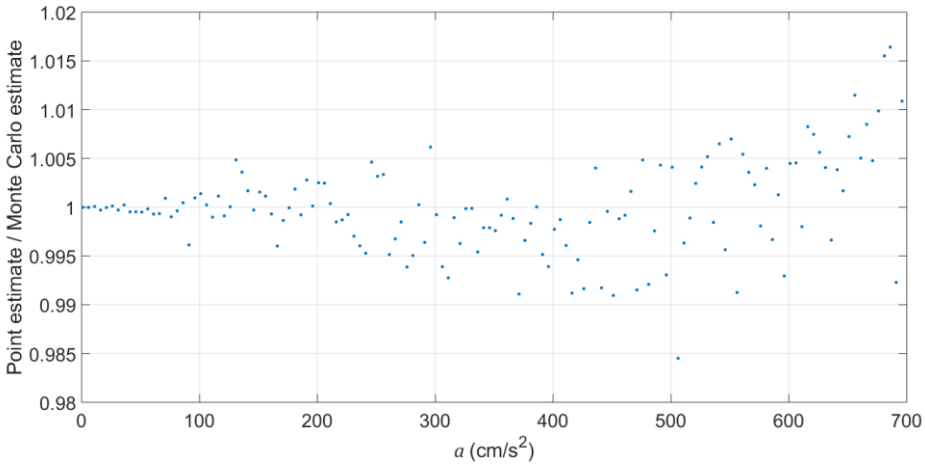

c) Both parameters considered uncertain

Figure 4.11 Case (2): Comparison between the mean point estimates of the annual exceedance rates with estimates from 250,000 Monte Carlo simulations; CV=0.40

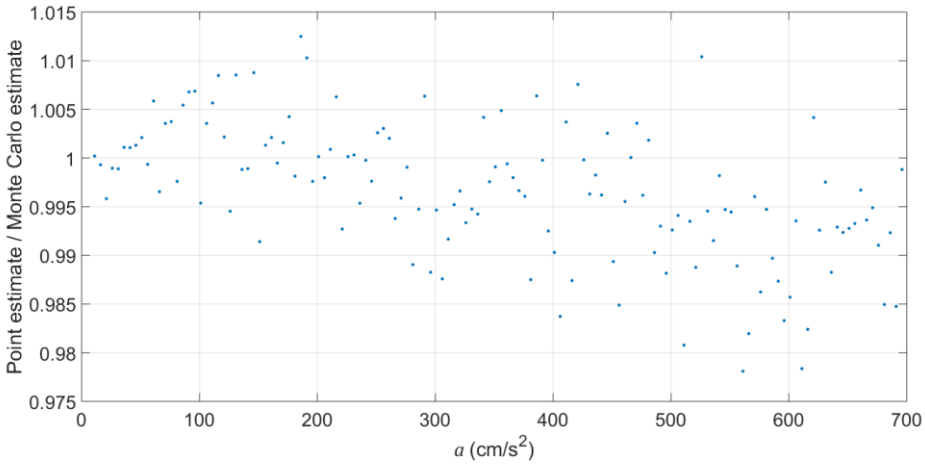

a) Uncertainty in parameter β

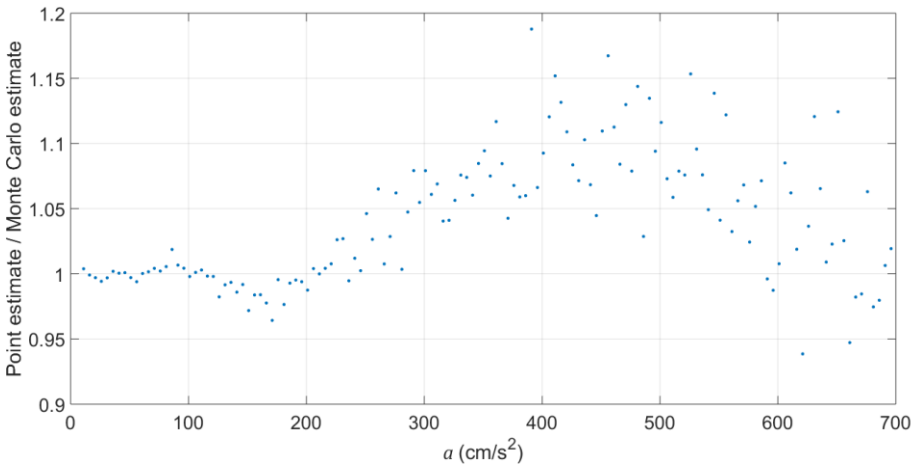

b) Uncertainty in parameter σ

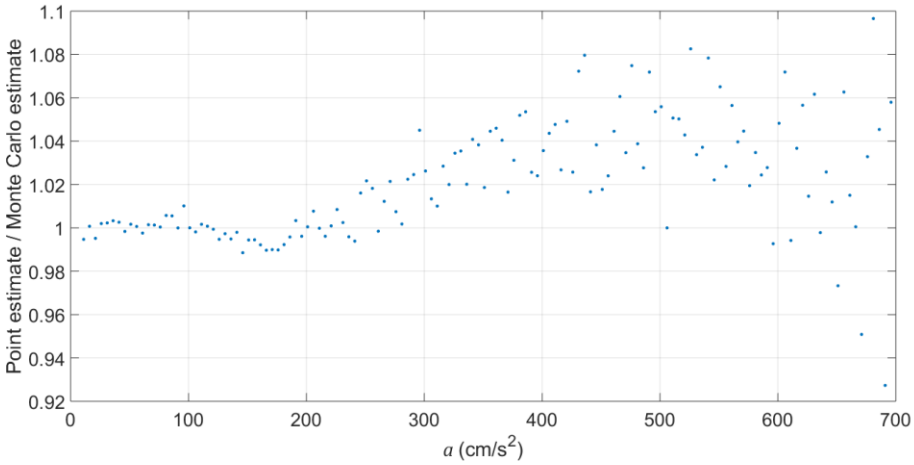

c) Both parameters considered uncertain

Figure 4.12 Case (2): Comparison between the variance point estimates of the annual exceedance rates with estimates from 250,000 Monte Carlo simulations; CV=0.40

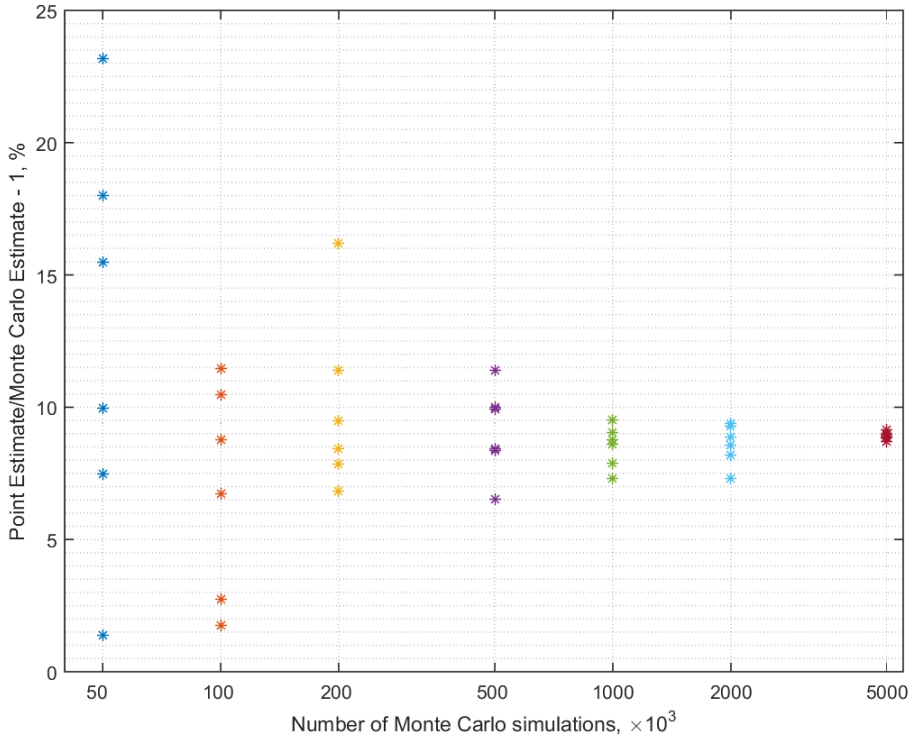

Figure 4.13 Case (2): Comparison of variance point estimates for varying sizes of Monte Carlo simulation ensembles; PGA=391 Gal

Analyses considering other combinations of mean values for parameters β and σ were also performed. As discussed in the literature review, β may take values in the range of 1.5 to 2.5, depending on the environment or the conditions of the source, while for σ, values in the range of 0.3 to 0.7 may represent the quality or degree of accuracy of ground motion prediction models. Results for various mean values of β and σ, and coefficients of variation equal to 20% and 40%, when each parameter is considered uncertain are shown in Figure 4.14 and Figure 4.15. A decrease in the annual exceedance rate curves for the range of small accelerations can be observed. This can be associated to the effect observed for smaller magnitude event ranges when plotting on logarithmic scale the Gutenberg-Richter relation, where at low magnitudes the plot becomes flatter, and this can be largely caused by the incompleteness of any data set due the inability to detect and characterize small events. Assigning a greater mean value to β decreases the expected number of seismic events per year that will exceed a certain intensity a. This is reflected in the annual exceedance rate curves having a steeper slope. It can also be observed that as the mean value assigned to parameter σ increases, the annual probability of exceeding an earthquake of a given PGA also increases. This is reasonable to expect since σ measures the uncertainty with which the natural logarithm of the peak ground acceleration is calculated. As the mean value of σ takes higher values, the uncertainty in σ produces a more noticeable effect on the uncertainty of the annual exceedance rates than that when uncertainty in β is considered. When high coefficients of variation are considered, the uncertainty in the annual exceedance rates is more sensitive to the uncertainty in parameter σ than it is to that in β.

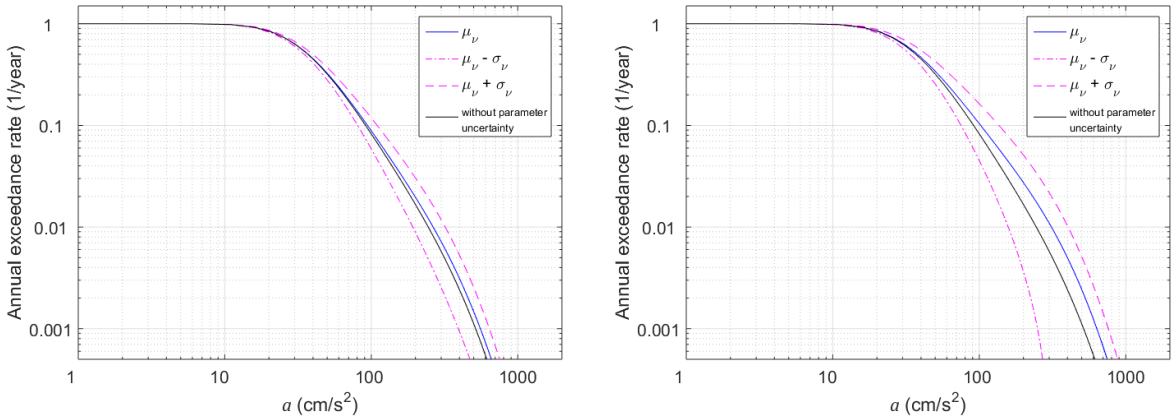

a) $E[\beta] = 1.5$, CV=0.20 b) $E[\beta] = 1.5$, CV=0.40

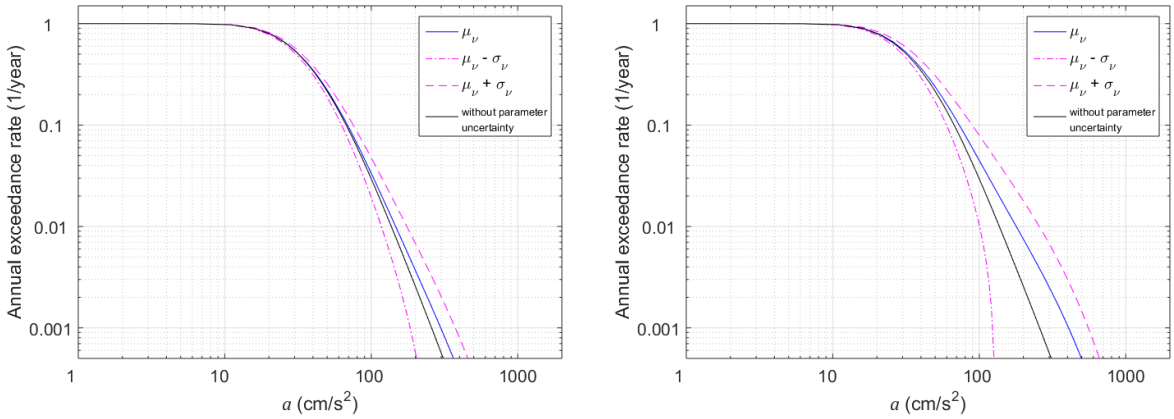

c) $E[\beta] = 2.5$, CV=0.20 d) $E[\beta] = 2.5$, CV=0.40

Figure 4.14 Case (2): Uncertainty in the annual exceedance rates due to uncertainty in parameter $\boldsymbol{\beta}$; $\boldsymbol{\sigma = 0.5}$

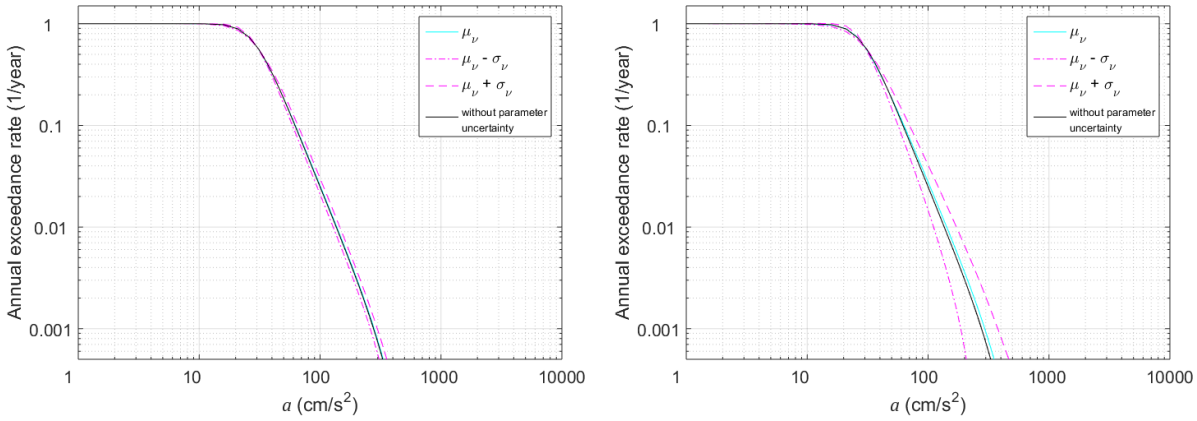

a) $E[\sigma] = 0.3$, CV=0.20 b) $E[\sigma] = 0.3$, CV=0.40

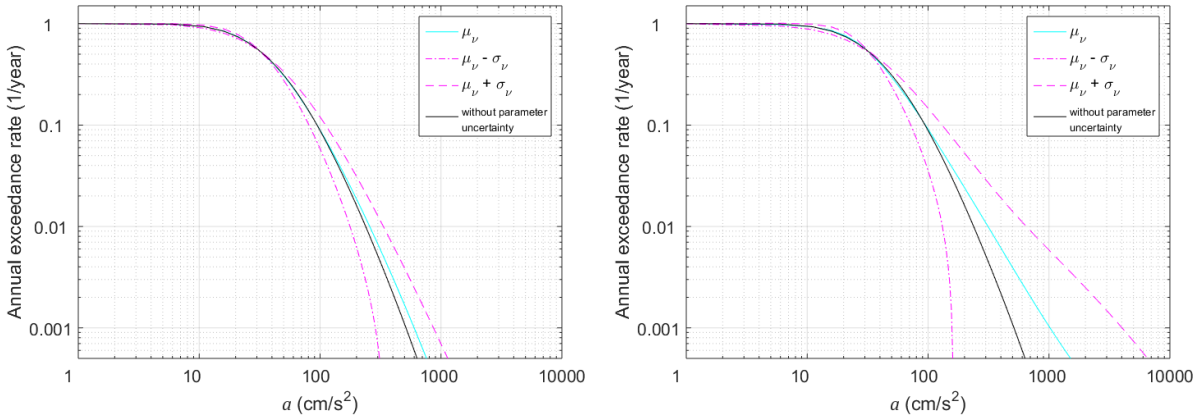

c) $E[\sigma] = 0.7$, CV=0.20 d) $E[\sigma] = 0.7$, CV=0.40

Figure 4.15 Case (2): Uncertainty in the annual exceedance rates due to uncertainty in parameter σ; $\beta = 2.0$

4.4 CASE (3): CIRCULAR SOURCE, PROBABILISTIC ATTENUATION RELATION

The analysis was performed using the analytical solution given in equation (2.11) considering parameters β and σ to be lognormally distributed, with mean value equal to 2.0 and 0.5, respectively, coefficients of variation of 10%, 20% and 40%, maximum radius $R_{\max} = 30$ km and depth $H = 30$ km. The variation of the mean exceedance rate, μ_v, as a function of the coefficients of variation is shown in Figure 4.16. Results considering the uncertainty in β and 10% coefficient of variation are very similar to the ones without parameter uncertainty, whereas for uncertainty in σ that is the case for coefficients of variation equal to 10% and 20%.

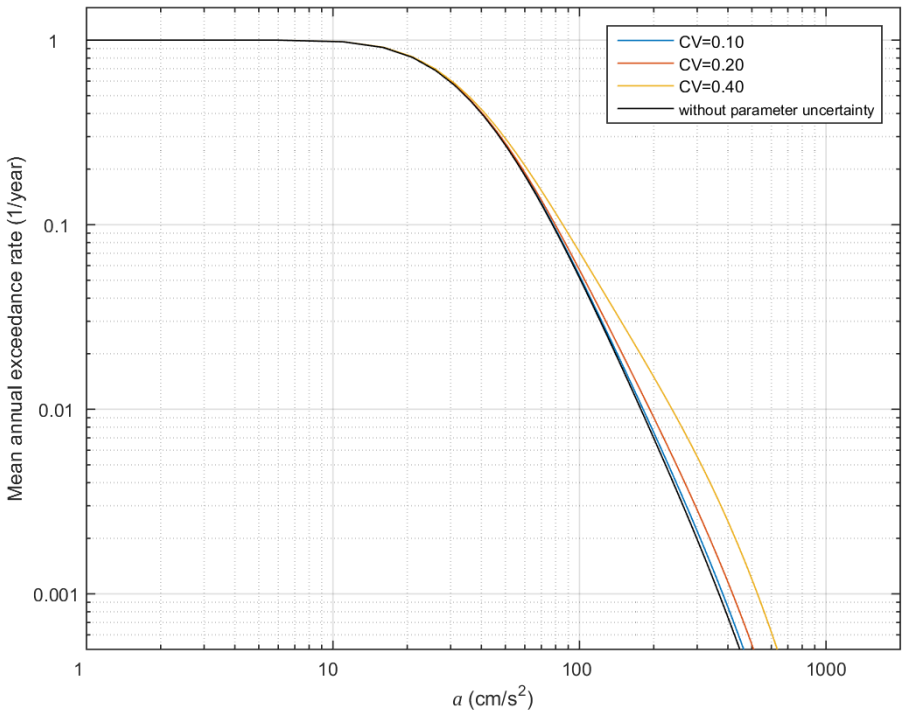

a) Uncertainty in parameter β

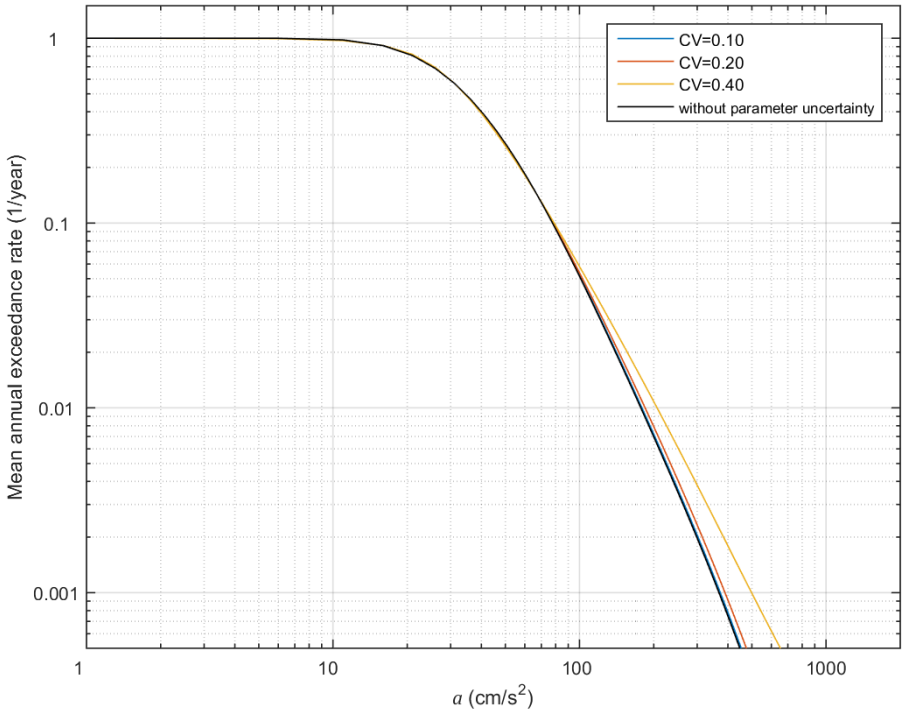

b) Uncertainty in parameter σ

Figure 4.16 Case (3): Influence of parameter uncertainty on the mean annual exceedance rate

The effect of considering uncertainty in both parameters β and σ is shown in Figure 4.17 for 20% coefficients of variation. Considering two sources of uncertainty adds up and increases the effect of parameter uncertainty compared to the previous cases in Figure 4.16. In this case the influence of parameter β is greater than that of σ. Table 4.8 summarizes PGA values for return periods of interest; e.g., for a 500-year event PGA values when uncertainty in β, in σ, and in both parameters is considered increase by about 15%, 5% and 20%, respectively. In the case of a nominal 100-year return period, the effect of accounting for parameter uncertainty are corresponding increments of PGA values of the order of 10%, 5%, and 15%.

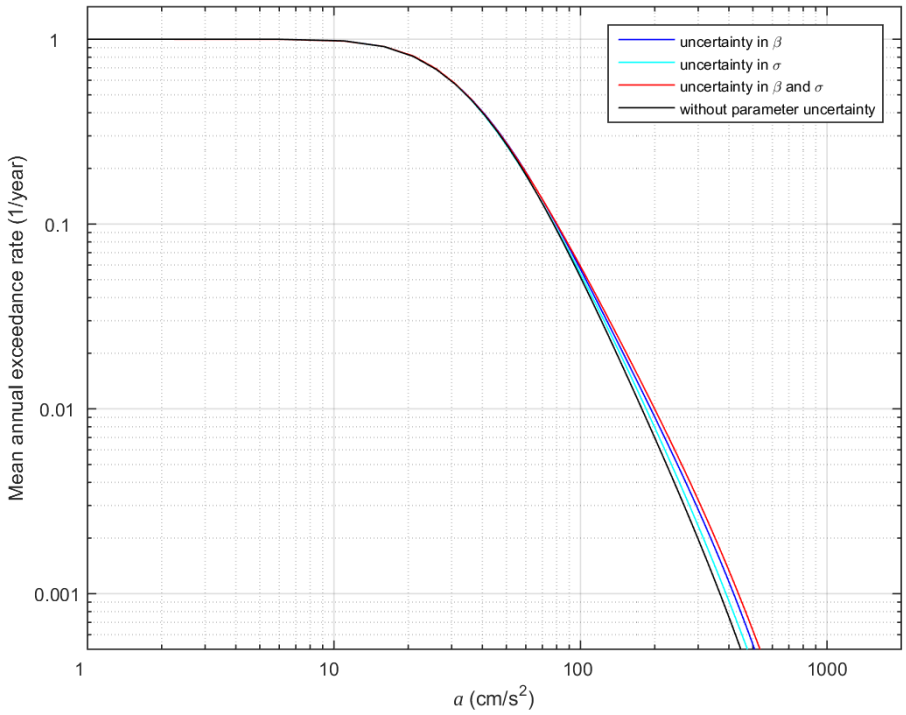

Figure 4.17 Case (3): Effect of parameter uncertainty on the mean annual exceedance rate; $E[\beta] = 2.0$, $E[\sigma] = 0.5$ and CV=0.20

Table 4.8 Case (3): Peak ground acceleration values from μ_v for some return periods; $E[\beta] = 2.0$, $E[\sigma] = 0.5$ and CV=0.20

Mean annual exceedance rate (1/year)	Return period (year)	Peak ground acceleration (Gal)			
		Without parameter uncertainty	Uncertainty in β	Uncertainty in σ	Uncertainty in β and σ
		μ_v	μ_v	μ_v	μ_v
0.020	50	140	149	144	154
0.010	100	177	193	185	200
0.002	500	299	337	315	352
0.001	1000	368	418	389	437

Figure 4.18 shows the variation of the mean annual exceedance rate, μ_v, and the mean plus/minus one standard deviation, $\mu_v \pm \sigma_v$. Table 4.9 lists PGA values from Figure 4.18 for some return periods. As for the mean μ_v, the effect of parameter uncertainty on σ_v is greater when uncertainty in both β and σ is taken into account. For a 500-year return period, PGA=299 Gal without including parameter uncertainty; the PGA from $\mu_v + \sigma_v$ are 415, 376 and 451 Gal, which amount to increments of the order of 40%, 25% and 50%, for uncertainty in β, in σ, and in both parameters, respectively. For a 100-year return period seismic event, the corresponding effect amounts to increments of about 35%, 20%, and 40%, respectively.

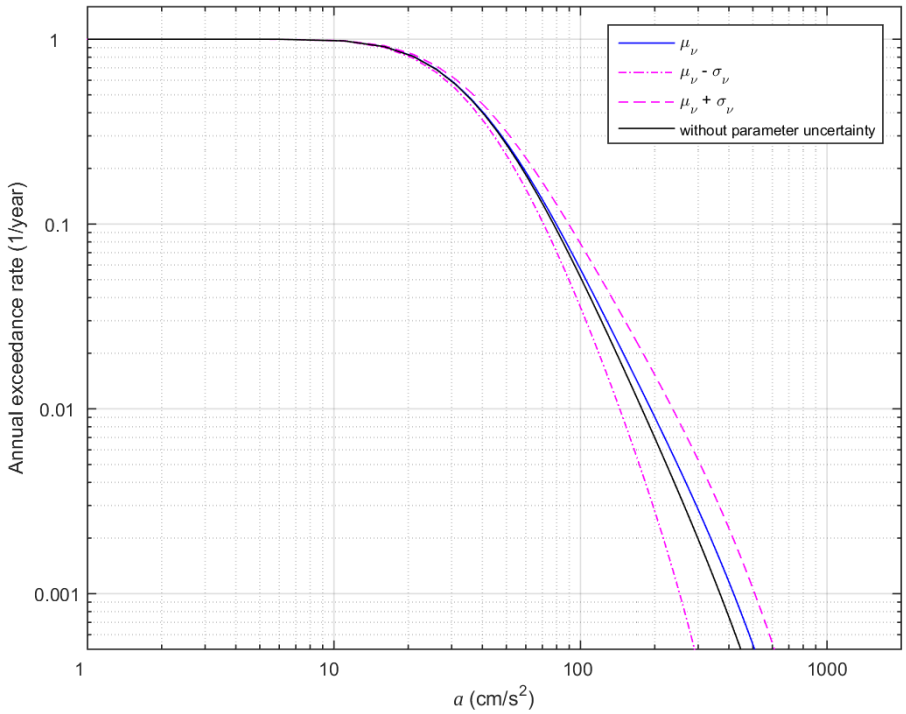

a) Uncertainty in parameter β

Figure 4.18 Case (3): Uncertainty in the annual exceedance rates due to parameter uncertainty; $E[\beta] = 2.0$, $E[\sigma] = 0.5$ and CV=0.20

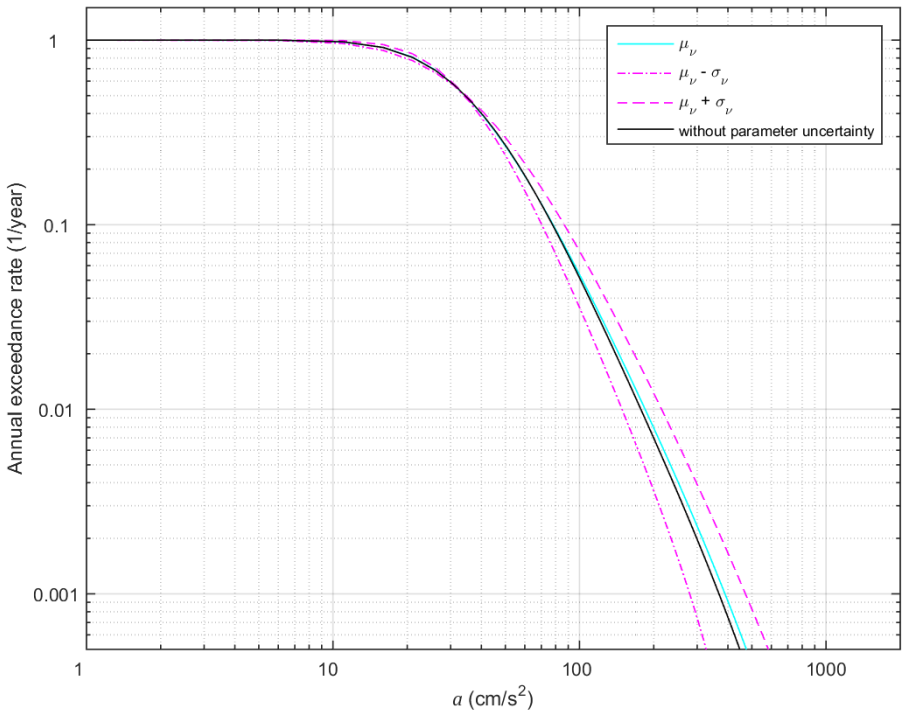

b) Uncertainty in parameter σ

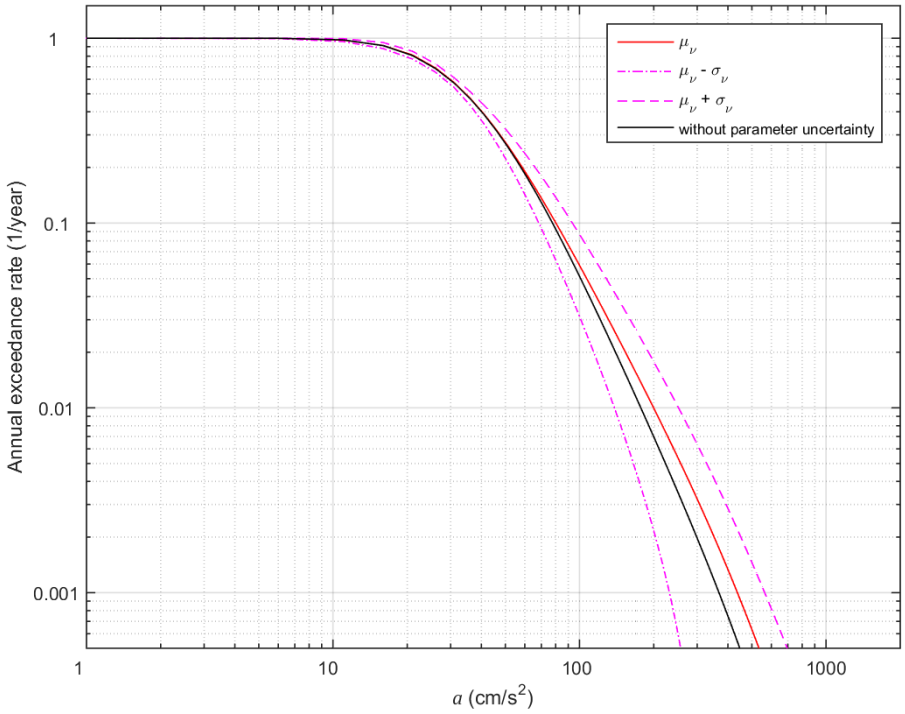

c) Both parameters considered uncertain

Figure 4.18 – Continued

Table 4.9 Case (3): Peak ground acceleration values from $\mu_v \pm \sigma_v$ for some return periods; $E[\beta] = 2.0$, $E[\sigma] = 0.5$ and CV=0.20

Annual exceedance rate (1/year)	Return period (year)	Peak ground acceleration (Gal)						
		Without parameter uncertainty	Uncertainty in β		Uncertainty in σ		Uncertainty in β and σ	
			$\mu_v - \sigma_v$	$\mu_v + \sigma_v$	$\mu_v - \sigma_v$	$\mu_v + \sigma_v$	$\mu_v - \sigma_v$	$\mu_v + \sigma_v$
0.020	50	140	119	179	120	166	114	190
0.010	100	177	144	236	149	215	139	252
0.002	500	299	216	415	235	376	203	451
0.001	1000	368	252	509	280	471	232	564

Comparisons between estimates of the mean and variance of the annual exceedance rate using the point estimates approach and 250,000 Monte Carlo simulations are shown in Figure 4.19 and Figure 4.20. The point estimate method performs well and yields results with very good accuracy. Mean estimates differ less than about 0.5%; estimates of the variance are within 2%, 5% and 2.5% when uncertainty is considered in β, σ, and both parameters, respectively.

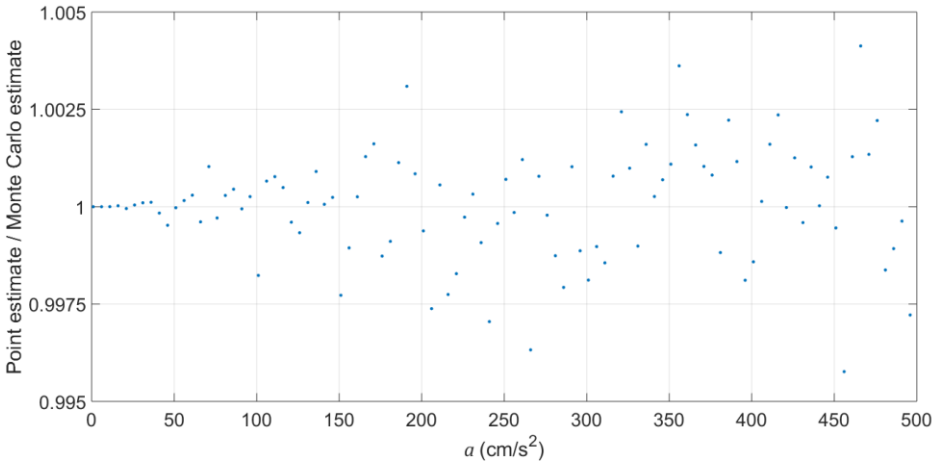

a) Uncertainty in parameter β

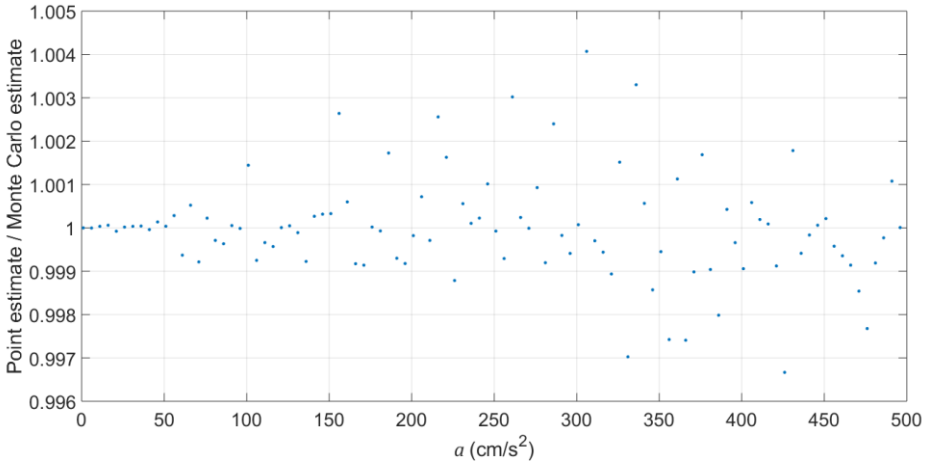

b) Uncertainty in parameter σ

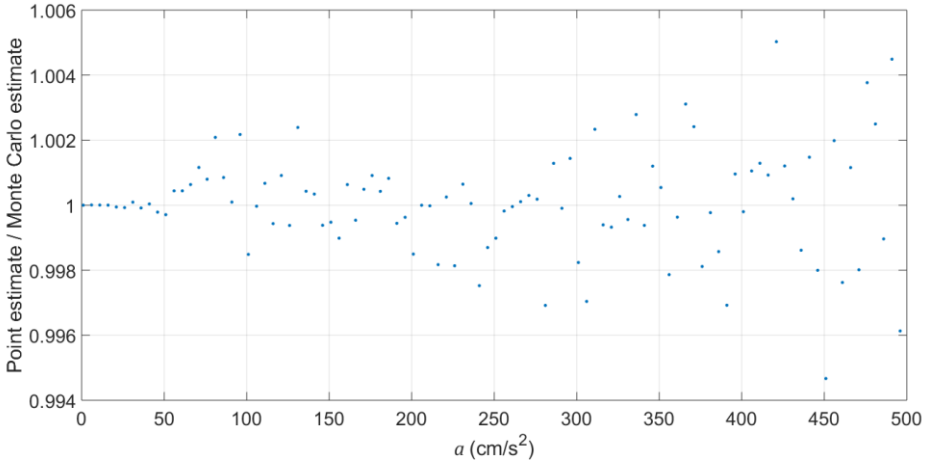

c) Both parameters considered uncertain

Figure 4.19 Case (3): Comparison between the mean point estimates of the annual exceedance rate with estimates from 250,000 Monte Carlo simulations; CV=0.20

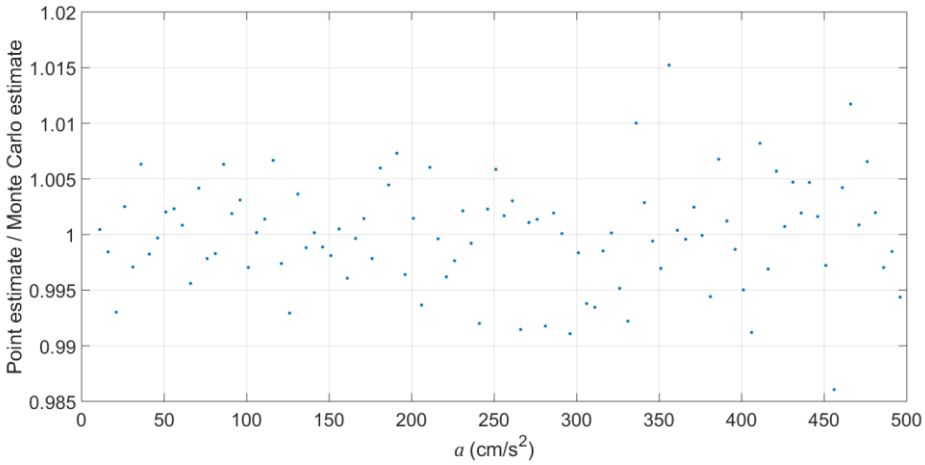

a) Uncertainty in parameter β

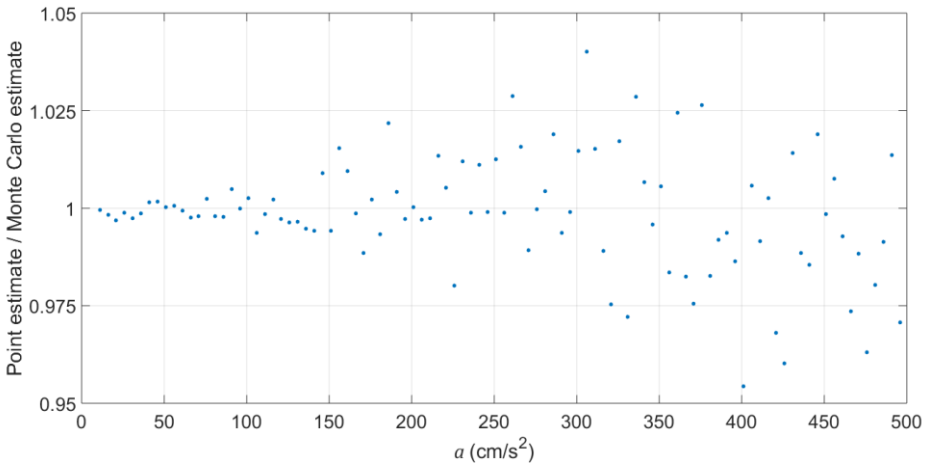

b) Uncertainty in parameter σ

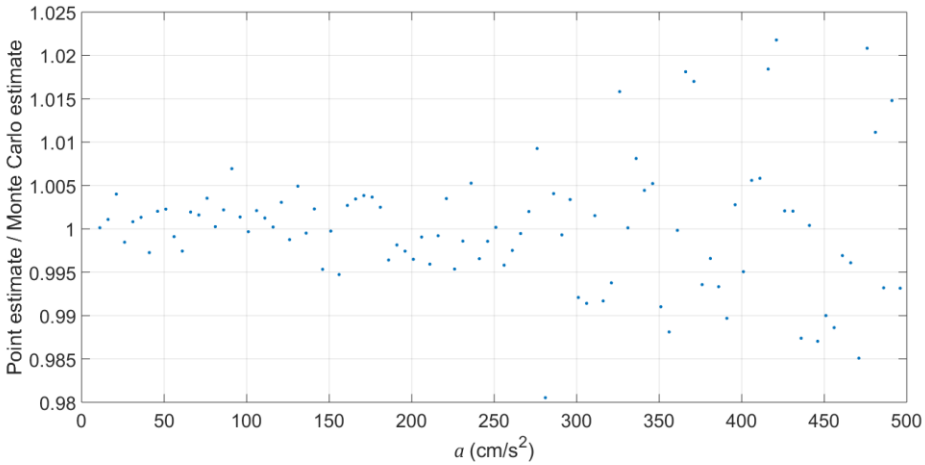

c) Uncertainty in both parameters

Figure 4.20 Case (3): Comparison between the variance point estimates of the annual exceedance rate with estimates from 250,000 Monte Carlo simulations; CV=0.20

Results for 40% coefficients of variation in β and σ are shown in Figure 4.21 and Table 4.10. The overall effect of parameter uncertainty is greater now. For 500-year return period, PGA values for the mean and the mean plus one standard deviation of the exceedance rate are about 65% and 220% greater than the case when parameter uncertainty is not considered; and 50% and 135% greater for 100-year return period.

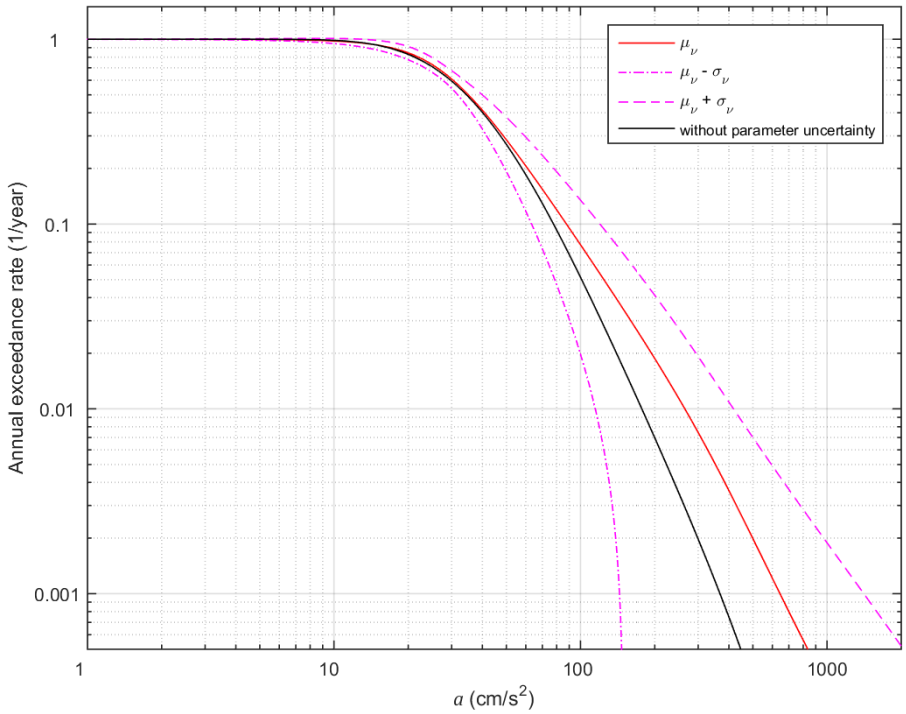

Figure 4.21 Case (3): Uncertainty in the annual exceedance rates due to parameter uncertainty; $E[\beta] = 2.0$, $E[\sigma] = 0.5$ and CV=0.40

Table 4.10 Case (3): Peak ground acceleration values from μ_v and $\mu_v \pm \sigma_v$ for some return periods; $E[\beta] = 2.0$, $E[\sigma] = 0.5$ and CV=0.40

Mean annual exceedance rate (1/year)	Return period (year)	Peak ground acceleration (Gal)			
		Without parameter uncertainty	Uncertainty in both parameters, β and σ		
			μ_v	$\mu_v - \sigma_v$	$\mu_v + \sigma_v$
0.020	50	140	194	100	294
0.010	100	177	265	115	417
0.002	500	299	499	139	968
0.001	1000	368	644	144	1410

A comparison between the mean and variance estimates of the annual exceedance rate and estimates based on 2×10^6 Monte Carlo simulations are illustrated in Figure 4.22. Mean estimates differ by less than 1%. In the case of the variance estimates differ by less than 6%. The PGA value that produced the highest difference between the variance estimates was equal to 441 Gal, for which an analysis was performed to estimate the variance based on a greater number of Monte Carlo simulations. Five repetitions of 5×10^6 simulations were computed for such value reducing the intensive computing time demanded by the complexity of the analytical solution involved in this case. Again, the results verified that as the number of simulations increases the variance estimates computed by the Monte Carlo method tends to stabilize around a certain value. For 5×10^6 simulations the difference between variance estimates is 4% for the PGA value representing the highest error between the methods.

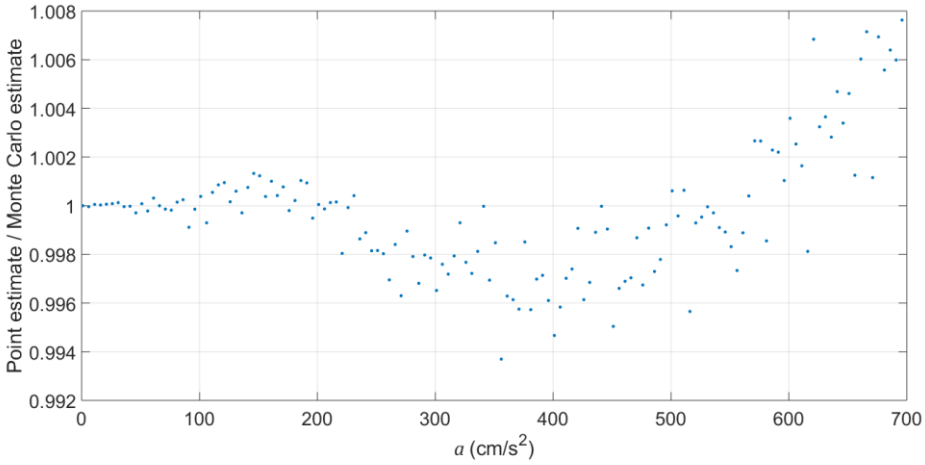

a) Mean

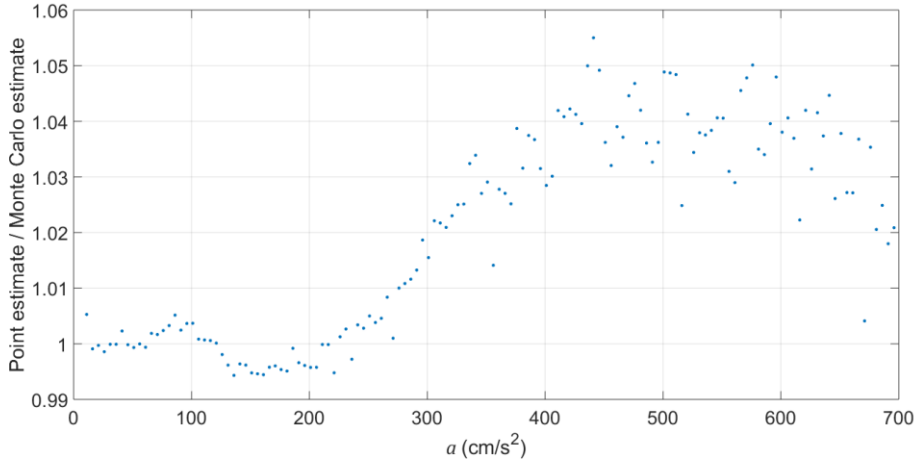

b) Variance

Figure 4.22 Case (3): Comparison between the mean and variance point estimates of the annual exceedance rate with estimates from 2×10^6 Monte Carlo simulations; CV=0.40

Finally, a series of combinations were examined taking into account the mean value of parameter β equal to 1.5 and 2.5; the mean value of parameter σ equal to 0.3 and 0.7, and considering coefficients of variation equal to 20% and 40%. The results are shown in Figure 4.23 to Figure 4.24. Similar trends as before can be observed.

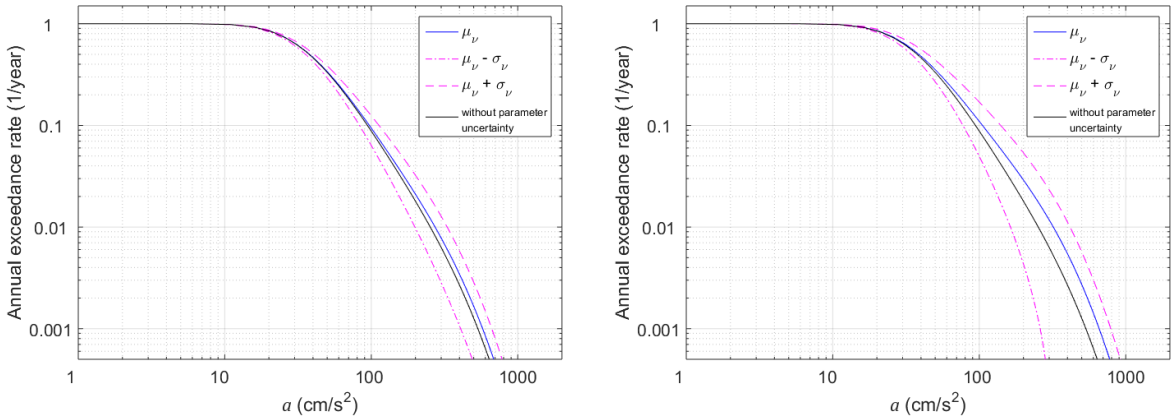

a) $E[\beta] = 1.5$, CV=0.20 b) $E[\beta] = 1.5$, CV=0.40

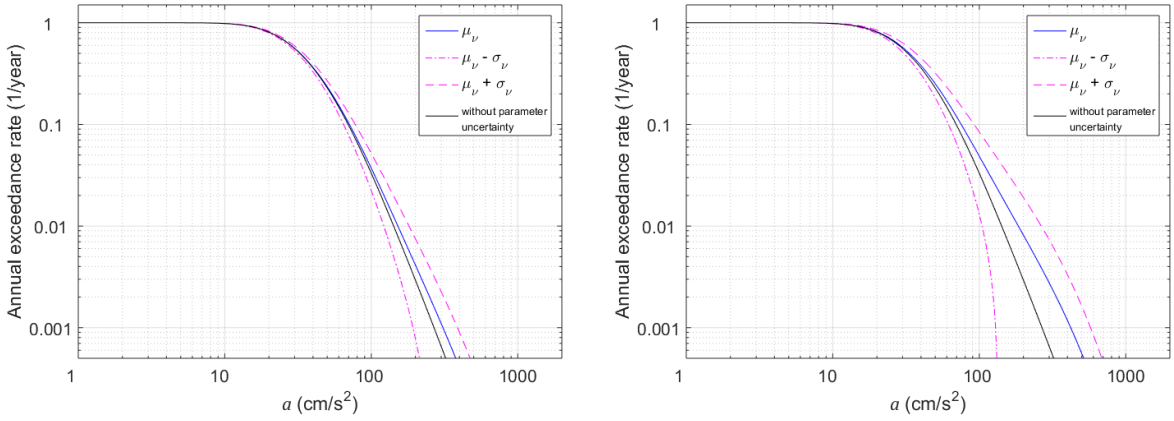

c) $E[\beta] = 2.5$, CV=0.20 d) $E[\beta] = 2.5$, CV=0.40

Figure 4.23 Case (3): Uncertainty in the annual exceedance rates due to uncertainty in parameter $\boldsymbol{\beta}$; $\boldsymbol{\sigma = 0.5}$

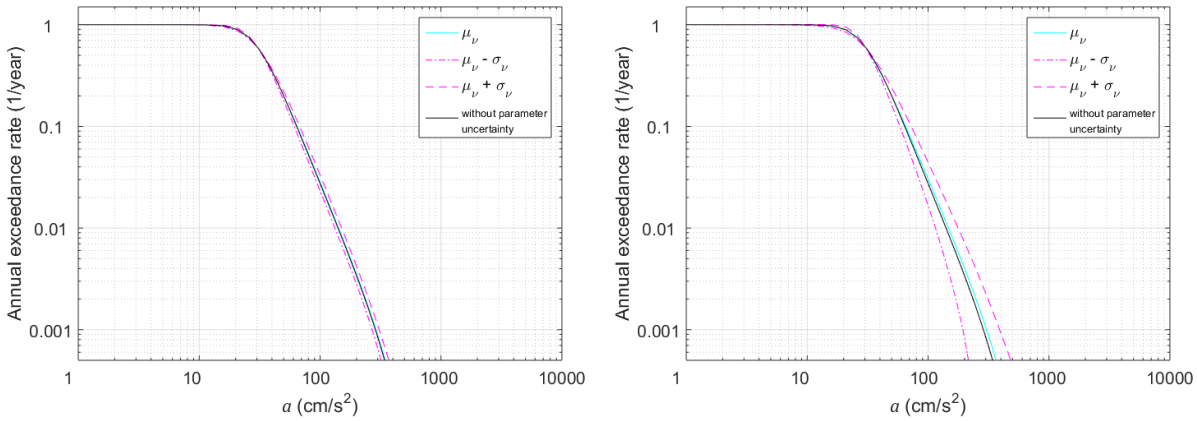

a) $E[\sigma] = 0.3$, CV=0.20 b) $E[\sigma] = 0.3$, CV=0.40

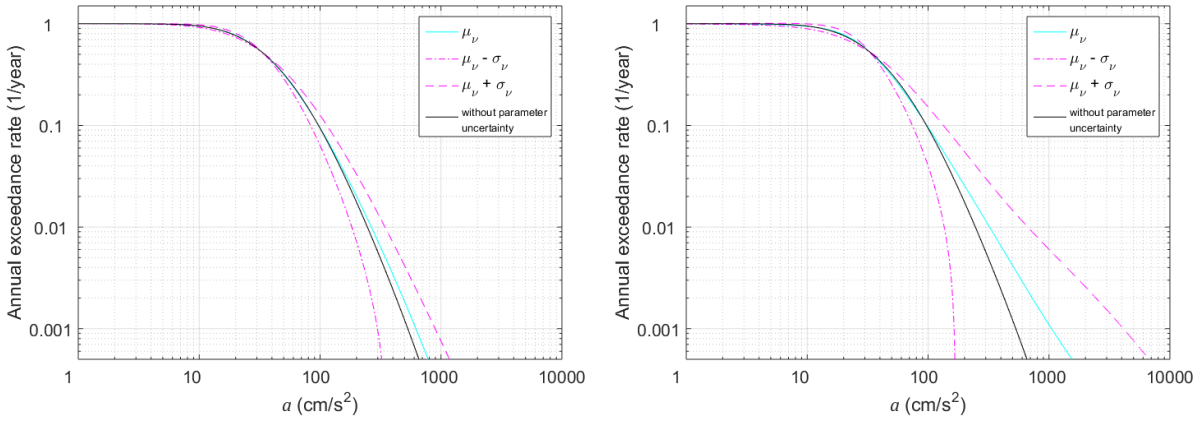

c) $E[\sigma] = 0.7$, CV=0.20 d) $E[\sigma] = 0.7$, CV=0.40

Figure 4.24 Case (3): Uncertainty in the annual exceedance rates due to uncertainty in parameter σ; $\beta = 2.0$

CHAPTER 5
CONCLUSIONS

A study has been presented to assess the uncertainty in probabilistic seismic hazard analysis (PHSA) due to the statistical uncertainty in some of the parameters involved in the magnitude distribution model and the ground motion intensity model. The uncertainty in the model parameters results from their statistical estimation using historical data. The work has focused on estimating the mean value and the variance of the annual exceedance rate of peak ground acceleration (PGA). An improved point estimate method based on the Rosenblatt transformation was used. Its main advantage over traditional approaches is that the estimating points and weights are readily defined and can be easily increased for accuracy if necessary. Monte Carlo simulations were used to assess the accuracy of point estimation. Three case studies were examined for which analytical solutions are available: (1) point source with deterministic median attenuation relation; (2) point source with probabilistic attenuation relation; and (3) circular source with probabilistic attenuation relation. Statistical uncertainty in two parameters has been considered: the slope related parameter β in the Gutenberg-Richter magnitude distribution model and the standard deviation σ of the natural logarithm of PGA in the ground motion intensity model. The statistics used for the uncertain parameters in the case studies were supported by an extensive literature review of real case studies. Some of the main findings from the analyses are:

- The effect of statistical uncertainty on the calculation of PGA values for return periods of interest may be significant. The effect was assessed in terms of the increase in PGA when comparing the mean annual exceedance rate, μ_v, and the mean plus one standard deviation, $\mu_v + \sigma_v$, against results from PSHA without including parameter uncertainty. For instance, for case (2), considering 20% coefficients of variation, PGA values for μ_v and $\mu_v + \sigma_v$ represent an increase of about 13-18% and 43-50%, for return periods between 100 and 500 years, respectively. If coefficients of variation equal to 40% were considered, such percentages are about 50-70% and 135-230%, respectively.
- The point estimate method using 5 points yields estimates of the mean and the variance of the annual exceedance rate with very good accuracy for return periods of engineering interest. It becomes less accurate for estimating the variance when large parameter uncertainty is considered, say about 40% coefficients of variation. The number of estimating points can be readily increased in such cases for greater accuracy.
- The complexity of the analytical solutions is an issue of relatively minor importance in terms of computing time; both the mean and the variance of the mean exceedance rate can be computed efficiently in short times using the point estimate method.

Being able to characterize the effect of parameter uncertainties in PSHA should be useful to assess the benefit of reducing such uncertainties by means of gathering additional information. This benefit can then be compared against the cost of gathering more information for the purpose of optimal decision making. Provided the point estimates methodology presented here for the assessment of the effect of parameter uncertainty is relatively easy to implement, its application could also be extended to other topics in structural engineering and reliability in which the need to quantify the impact of poor or insufficient information about some of the parameters involved in the problems under study is not infrequent. Future studies may deal with the assessment of parameter uncertainty on other intensity measures such as spectral accelerations and its effect in the computation of uniform hazard spectra. The influence of uncertainties in parameters of more complex seismic source models could also be studied. The formulation presented in this work could be extended as well for the assessment of parameter uncertainty in formulations for joint hazard analysis of multiple intensity measures and ground motion parameters.

REFERENCES

Aki, K. (1965). Maximum likelihood estimate of b in the formula logN=a-bM and its confidence limits. *Bulletin of the Earthquake Research Institute, Tokyo University, 43*, 237-239.

Baker, J. W. (2013). Probabilistic Seismic Hazard Analysis. *White Paper Version 2.0*, 79.

Bender, B. (1983). Maximum likelihood estimation of b values for magnitude grouped data. *Bulletin of the Seismological Society of America, 73*(3), 831-851.

Bird, P., & Kagan, Y. Y. (2004). Plate-tectonic analysis of shallow seismicity: Apparent boundary width, beta, corner magnitude, coupled lithosphere thickness, and coupling in seven tectonic settings. *Bulletin of Seismological Society of America, 94*(6), 2380-2399.

Boore, D. M., Joyner, W. B., & Fumal, T. E. (1997). Equations for estimating horizontal response spectra and peak acceleration from western North American Earthquakes: A summary of recent work. *Seismological Research Letters, 68*(1), 128-153.

Cornell, C. A. (1968). Engineering seismic risk analysis. *Bulletin of the Seismological Society of America, 58*(5), 1583-1606.

Cornell, C. A., & Vanmarcke, E. H. (1969, January). The major influences on seismic risk. *4th World Conference on Earthquake Engineering.* Santiago de Chile.

Cornell, C. A., Banon, H., & Shakal, A. F. (1979). Seismic motion and response prediction alternatives. *Earthquake Engineering and Structural Dynamics, 7*(4), 295-315.

Der Kiureghian, A., & Ditlevsen, O. (2009). Aleatory or epistemic? Does it matter? *Structural Safety, 31*, 105-112.

Douglas, J. (2017). *Ground motion prediction equations 1964-2016*. Retrieved from http://www.gmpe.org.uk

Dowrick, D. (1987). *Earthquake Resistant Design: For Engineers and Architects.* Chichester: John Wiley & Sons, Ltd.

Esteva, L. (1967, July). Criteria for the construction of spectra for seismic design. *3rd Panamerican Symposium on Structures.* Caracas, Venezuela.

González de Vallejo, L. I., García-Mayordomo, J., & Insua, J. M. (2006). Probabilistic seismic-hazard assessment of the Canary Islands. *Bulletin of the Seismological Society of America, 96*(6), 2040-2049. doi:10.1785/0120050139

Gorman, M. R. (1980). *Reliability of structural systems.* PhD Thesis, Case Western Reserve University, Cleveland, Ohio.

Grünthal, G., & Wahlström, R. (2001). Sensitivity of parameters for probabilistic seismic hazard analysis using a logic tree approach. *Journal of Earthquake Engineering, 5*(3), 309-328. doi:10.1142/S1363246901000376

Gutenberg, B., & Richter, C. F. (1954). *Seismicity of the Earth and Associated Phenomena* (2nd ed.). Princeton, New York: Princeton University Press.

Isacks, B., & Oliver, J. (1964). Seismic waves with frequencies from 1 to 100 cycles per second recorded in a deep mine in northern New Jersey. *Bulletin of the Seismological Society of America, 54*(6), 1941-1979.

JCSS. (2001). *Probabilistic Model Code for Probability Based Design.* The Joint Committee on Structural Safety.

Kagan, Y. Y. (2002). Seismic moment distribution revisited: I. Statistical results. *Geophysical Journal International, 148*, 520-541.

Leyton, F., Ruiz, S., & Sepúlveda, S. A. (2009). Preliminary re-evaluation of probabilistic seismic hazard assessment in Chile: From Arica to Taitao Peninsula. *Advances in Geosciences, 22,* 147-153.

McGuire, R. K. (1974). *Seismic structural response risk analysis, incorporating peak response regressions on earthquake magnitude and distance.* Research report R74-51, Massachusetts Institute of Technology (MIT), Department of Civil Engineering, Cambridge, Massachusetts.

Mogi, K. (1962). Magnitude-frequency relation for elastic shocks accompanying fractures of various materials and some related problems in earthquakes (2nd Paper). *Bulletin of the Earthquake Research Institute, 40,* 831-853.

Ordaz, M. (2004). Some integrals useful in probabilistic seismic hazard analysis. *Bulletin of the Seismological Society of America, 94*(4), 1510-1516.

Ordaz, M., Jara, J. M., & Singh, S. K. (1989). *Seismic risk and design spectra for the State of Guerrero.* UNAM, Institute of Engineering.

Reiter, L. (1990). *Earthquake hazard analysis: issues and insights.* New York: Columbia University Press.

Rosenblueth, E. (1975). Point estimates for probability moments. *Proc. Nat. Acad. Sci. USA, 72*(10), 3812-3814.

Sen, T. K. (2009). *Fundamentals of Seismic Loading on Structures.* United Kingdom: John Wiley & Sons, Ltd.

Shi, Y., & Bolt, B. A. (1982). The standard error of the magnitude-frequency b value. *Bulletin of the Seismological Society of America, 72*(5), 1677-1687.

Stirling, M., McVerry, G., Berryman, K., McGinty, P., Villamor, P., Van Dissen, R., . . . Sutherland, R. (2000). *Probabilistic seismic hazard assessment of New Zealand.* Institute of Geological and Nuclear Sciences, Earthquake Commission Research Foundation.

Strasser, F. O., Abrahamson, N. A., & Bommer, J. J. (2009). Sigma: Issues, insights, and challenges. *Seismological Research Letters, 80*(1), 40-56. doi:10.1785/gssrl.80.1.40

Utsu, T. (1965). A method for determining the value of b in the formula logN=a-bM showing the magnitude-frequency relation for earthquakes. *Geophysics Bulletin, Hokkaido University, 13*, 99-103.

Utsu, T. (1966). A statistical significance test of the difference in b-value between two earthquake groups. *Journal of Physics of the Earth*, *14*(2), 37-40.

Utsu, T. (2002). Statistical Features of Seismicity. In W. Lee, H. Kanamori, P. Jennings, & C. Kisslinger (Eds.), *International Handbook of Earthquake & Engineering Seismology* (Vol. 81A, pp. 719-732). Academic Press.

Wang, Z. (2010). Seismic hazard assessment: Issues and alternatives. *Pure and Applied Geophysics*. doi:10.1007/s00024-010-0148-3

Zhao, Y.-G., & Ono, T. (2000). New point estimates for probability moments. *Journal of Engineering Mechanics*, *126*(4), 433-436.

Zhao, Y.-G., & Ono, T. (2001). Moment methods for structural reliability. *Structural Safety*, *23*, 47-75.